D7.3 Medium-term impacts of cooperative, connected, and automated mobility on freight transport

Deliverable D7.3 – WP7 – PU

LEVITATE has received funding from the European Union's Horizon 2020 research and innovation programme under grant agreement No 824361.

D7.3 Medium-term impacts of cooperative, connected, and automated mobility on freight transport

Work package 7, Deliverable D7.3

Please refer to this report as follows:
Hu, B., Brandstätter, G., Ralbovsky, M., Kwapisz, M., Vorwagner, A., Zwart, R.d., Mons, C., Weijermars, W., Roussou, J., Oikonomou, M., Ziakopoulos, Chaudhry, A., Sha, S., Haouari, R., Boghani, H.C., (2021). *Medium-term impacts of cooperative, connected, and automated mobility on freight transport, Deliverable D7.3 of the H2020 project LEVITATE.

Project details:	
Project start date: **Duration:** **Project name:**	01/12/2018 42 months LEVITATE – Societal Level Impacts of Connected and Automated Vehicles
Coordinator:	Andrew Morris, Prof. of Human Factors in Transport Safety Loughborough University Ashby Road, LE11 3TU Loughborough, United Kingdom
	This project has received funding from the European Union's Horizon 2020 research and innovation programme under grant agreement No 824361.

Deliverable details:	
Version: **Dissemination level:** **Due date:** **Submission date:**	Final PU 31/10/2021 3/11/2021

*The original title of this deliverable was "The medium-term impact, cost and benefits of cooperative and automated freight transport". The title has been revised to better reflect the current terminology used in this field of research.

Lead contractor for this deliverable:
AIT

Report Author(s):	Hu, B., Brandstätter, G., Ralbovsky, M., Kwapisz, M., Vorwagner, A. (AIT), Austria Zwart, R.d., Mons, C., Weijermars, W. (SWOV), The Netherlands Roussou, J., Oikonomou, M., Ziakopoulos (NTUA), Greece Chaudhry, A., Sha, S., Haouari, R., Boghani, H.C. (LOUGH), UK

Revision history

Date	Version	Reviewer	Description
26/10/2021	Preliminary draft 1	Pete Thomas, Amna Chaudhry (LOUGH)	Review round 1 – Accepted wit reservations
09/09/2021	Preliminary draft 1	Sebastien Glaser (QUT)	Review round 1 – Accepted wit reservations
3/11/2021	Final draft	Camellia Hayes Vanessa Millar	
3/11/2021	Final deliverable	Andrew Morris – Loughborough University ➔ EC	

Table of contents

Table of figures 1
Table of tables 3
Executive summary 4
1 Introduction 5
1.1 LEVITATE 5
1.2 Work package 7 and Deliverable 7.3 within LEVITATE 5
2 Sub-use cases 8
2.1 Automated urban delivery 8
2.2 Automated freight consolidation 9
2.3 Hub-to-hub automated transport 10
2.4 Truck platooning on urban highway bridges 11
3 Methods 12
3.1 Microscopic simulation 12
3.1.1 Automated urban delivery and automated consolidation 12
3.1.2 Hub-to-hub automated transport 16
3.2 Bridge modelling 18
3.2.1 Vertical traffic load effects on bridges 19
3.2.2 Horizontal traffic load effects on bridges 20
3.2.3 Assumptions 21
3.2.4 Simulation of traffic flow on bridges 23
3.2.5 Bridge response simulation 28
4 Obtained Impacts 32
4.1 Congestion 32
4.1.1 Automated urban delivery 32
4.1.2 Automated consolidation 34
4.1.3 Hub-to-hub automated transport 36
4.2 Platoonong on bridges impacts 37
4.2.1 No measures: reduction of structural safety 37
4.2.2 Bridge strengthening 44
4.2.3 Intelligent access control 47
5 Conclusion and future work 51
5.1 Conclusions 51
5.2 Future work 51
References 52

Table of figures

Figure 2.1: Function of the automated transfer hub. Human-operated trucks deliver the containers to the transfer hub (yellow arrow) and from there automated trucks carry them on to the highway (blue arrow). 11
Figure 3.1: Simulated area for route A. 13
Figure 3.2: Simulated area for route B. 13
Figure 3.3: Area in the southern of Vienna where we assumed the location of the transfer hub..... 17
Figure 3.4: Modelled area for the transfer hub in AIMSUN..... 17
Figure 3.5: Time-dependent traffic volume in Vienna. No data are available from 0:00-5:00 because of the minimal traffic volume on the road. In the simulation this was set to half of the amount of 23:00-24:00. 18
Figure 3.6: Scheme of an influence line for midspan bending moment of a two-span bridge, loaded with 4 axle forces. 19
Figure 3.7: Example of time-history of bridge cross-section force (left); Example of histogram of weekly maxima with fitted extreme-value distribution (right). 20
Figure 3.8: Comparison of quasi-static and dynamic history of the cross-section force (example). 20
Figure 3.9: Assumed cost of bridge strengthening (rough estimates). 22
Figure 3.10: Distribution (Cumulative Density Function) of gross vehicle weight for different vehicle types according, with added lower and upper bounds. 24
Figure 3.11: Example of vehicle-distance (axle-to-axle) distributions for traffic intensities from 0.1 to 0.5 vehicles/s with v_{fl}=80 km/h and L_v=15m..... 24
Figure 3.12: Change of traffic composition with increasing traffic amount. Mean time delay between vehicle passages (left); Composition of vehicle types in each lane (right). 26
Figure 3.13: Scheme of braking scenario at start (top) and end (bottom) of the braking maneuver..... 26
Figure 3.14: Example of influence lines of a simply-support single span beam with a span of 50 m. Influence on midspan bending moment (left) and shear force near the abutment (right)..... 28
Figure 3.15: Cross-section schemes of the considered bridge types. 29
Figure 3.16: Scheme of shifting of extreme value distributions to longer reference periods..... 30
Figure 3.17: Calculated Dynamic Amplification Factors for different levels of bending moment (left) and shear force (right) in a prestressed-concrete T-beam bridge with 20 m span (top), and in a steel box-girder bridge with 90 m span (bottom)..... 31
Figure 4.1: Delay (s/km) for the delivery vehicles in the simulation scenarios. 33
Figure 4.2: Delay (s/km) for the delivery vehicles in the delivery scenarios. 34
Figure 4.3: Delay (s/km) for the background traffic with and without transfer hub..... 36
Figure 4.4: Bending moment exceedance probabilities for traffic without congestions and daily traffic volume of 39000 vehicles, for traffic mixes A, B, C and D. 38
Figure 4.5: Shear force exceedance probabilities for traffic without congestions and daily traffic volume of 39000 vehicles, for traffic mixes A, B, C and D..... 38
Figure 4.6: Bending moment exceedance probabilities for traffic mix A with different vehicle distances in congestion..... 39
Figure 4.7: Shear force exceedance probabilities for traffic mix A with different vehicle distances in congestion. 39

Figure 4.8: Braking forces: 95%-quantiles of extreme-value-distribution with reference time period of 50 years. Traffic mix A with traffic volumes of 12000, 39000, 66000, 93000 and 120000 vehicles/day. 40
Figure 4.9: Braking forces: 95%-quantiles of extreme-value-distribution with reference time period of 50 years. Traffic mixes A, B, C, D with a traffic volume of 93000 vehicles/day. 41
Figure 4.10: Bending moment exceedance probabilities for traffic mix A, constant congestion distances (C_5), P_{cong}=0.99, P_{flow}=0.999, traffic volume of 39000 vehicles/day and different platooning penetration rates. 41
Figure 4.11: Shear force exceedance probabilities for traffic mix A, constant congestion distances (C_5), P_{cong}=0.99, P_{flow}=0.999, traffic volume of 39000 vehicles/day and different platooning penetration rates. 42
Figure 4.12: Bending moment exceedance probabilities for traffic mix A, traffic volume of 39000 vehicles/day, platooning penetration rate 60% and different congestion parameters. 43
Figure 4.13: Braking forces: 95%-quantiles of extreme-value-distribution with reference time period of 50 years. Traffic mix A with different platooning penetration rates. 43
Figure 4.14: Required increase of bending moment resistance in the traffic scenario with 60% platooning penetration rate, constant distances in congestion (C_5), P_{cong}=0.99 and traffic volume of 39000 vehicles/day. 45
Figure 4.15: Required increase of shear force resistance in the traffic scenario with 60% platooning penetration rate, constant distances in congestion (C_5), P_{cong}=0.99 and traffic volume of 39000 vehicles/day. 45
Figure 4.16: Rough cost estimates of required resistance increase in relation to cost of bridge replacement. 46
Figure 4.17: Bending moment exceedance probabilities for traffic mix A, traffic volume of 39000 vehicles/day, platooning penetration rate 60%, congestion distances $\mathcal{N}10{,}5$, P_{cong}=0.99, and different inter-vehicle distances within platoons. 48
Figure 4.18: Shear force exceedance probabilities for traffic mix A, traffic volume of 39000 vehicles/day, platooning penetration rate 60%, congestion distances $\mathcal{N}10{,}5$, P_{cong}=0.99, and different inter-vehicle distances within platoons. 48

Table of tables

Table 1.1: Overview of the impacts in WP7. Highlighted are the medium-term impacts for this deliverable..... 6
Table 2.1: Performance of the delivery scenarios and their main limiting factors (red). .. 9
Table 3.1: List of delivery scenarios for the automated delivery and automated consolidation SUCs. 14
Table 3.2: Scenarios for different CAV market penetration rates..... 15
Table 3.3: Districts of Vienna and their level of urbaness..... 15
Table 3.4: Vehicle parameters – adopted from report of Freundt et al. 2011. 23
Table 3.5: Constitution of traffic, adopted with modifications (Freundt et.al. 2011). 25
Table 3.6: Inter-vehicle axle distances in congestion, adopted with modifications from (Freundt et.al. 2011) 26
Table 3.7: Three examples of braking force calculation results 27
Table 3.8: Basic properties of analysed bridge models 29
Table 4.1: Delay (s/km) for the delivery vehicles in the simulation scenarios. The values under the simulation scenarios are CAV market penetration rates (manual vehices, 1st generation AVs, 2nd generation AVs). 32
Table 4.2: Delay (s/km) for the delivery vehicles in the delivery scenarios..... 33
Table 4.3: Results for different delivery scenarios taken from D7.2. 34
Table 4.4: Total delay for the delivery vehicles per day. 35
Table 4.5: Delay (s/km) for the background traffic in the simulation scenarios. 35
Table 4.6: Delay (s/km) for the background traffic with and without transfer hub. 36
Table 4.7: Analyzed inter-vehicle distances within platoons. 47
Table 4.8: Required inter-vehicle distances of platoons in intelligent access control. 49
Table 4.9: Delay (s/km) caused by intelligent access control for 50 km/h and 80 km/h cruising speed..... 50

Executive summary

The aim of the LEVITATE project is to prepare a new impact assessment framework to enable policymakers to manage the introduction of connected and automated transport systems, maximize the benefits and utilize the technologies to achieve societal objectives. As part of this work the LEVITATE project seeks to forecast societal level impacts of cooperative, connected and automated mobility (CCAM). This includes impacts on safety, environment, economy and society.

This report specifically focuses on freight transport, providing an analysis for the medium-term impacts of different freight transport concepts – also called "sub-use cases". The impacts to be studied have been defined in the Deliverable 3.1, which provided a preliminary taxonomy of the potential impacts of CCAM. The medium-term impacts presented in this report are those described as systemic impacts, which are congestion caused by freight traffic and the extensive topic of platooning impacts on bridges.

After an extensive literature review and a stakeholder reference group (SRG) workshop, a preliminary list of the urban transport sub-use cases was developed, presented in Deliverable 7.1. The proposed automated freight transport sub-use cases have been prioritized for their consideration in further investigation. During prioritization, factors such as widespread studies being followed on those sub-use cases and the feasibility of impact assessment have been considered. The sub-use cases that are presented in this report are on automated urban delivery, automated freight consolidation, hub-to-hub automated transport and truck platooning on urban highway bridges.

For assessing the congestion impacts of the first three sub-use cases, studies used micro-simulation methods applied toa smaller area of Vienna. The results show that the congestion caused by freight traffic to the overall road traffic is very low since their share of the traffic volume is minimal. Nevertheless, automated vehicles provide the ability to move freight transport during the off-peak hours and the night-time provides small traffic benefits to passenger transport during peak hours.

The extensive topic of truck platooning on urban highway bridges is discussed in this report, showing that the burden on bridges caused by truck platoons should not be underestimated. In order to minimize the failure probability, medium-term measures such as structural strengthening and intelligent access control should be considered. Finally, methods to assess their impacts are presented.

The key results obtained in this deliverable are: i) Impact on the congestion caused by freight traffic to the overall road traffic is small and ii) highway bridges must be prepared for the operation of truck platooning in order to minimise the structural damage. These results will be included in the final LEVITATE product which is the LEVITATE Policy Support Tool (PST).

1 Introduction

1.1 LEVITATE

Societal **Lev**el **I**mpacts of Connec**t**ed and **A**utoma**t**ed Vehicl**e**s (LEVITATE) is a European Commission supported Horizon 2020 project with the primary objective to prepare a new impact assessment framework to enable policymakers to manage the introduction of connected and automated transport systems, to maximise the benefits and to utilise the technologies to achieve societal objectives.

Specifically LEVITATE has four key objectives:

- To establish **a multi-disciplinary methodology** to assess the short, medium and long-term impacts of CCAM on mobility, safety, environment, society and other impact areas. Several quantitative indicators will be identified for each impact type.
- To develop a range of **forecasting and backcasting** scenarios and baseline conditions relating to the deployment of one or more mobility technologies that will be used as the basis of impact assessments and forecasts. These will cover three primary use cases – automated urban shuttle, passenger cars and freight services.
- To apply the methods and **forecast the impact of CCAM** over the short, medium and long term for a range of use cases, operational design domains and environments and an **extensive range of mobility, environmental, safety, economic and societal indicators**. A series of case studies will be conducted to validate the methodologies and to demonstrate the system.
- To incorporate the established methods within a **new web-based policy support tool** to enable city and other authorities to forecast impacts of CCAM on urban areas. The methods developed within LEVITATE will be available within a toolbox allowing the impact of measures to be assessed individually. A Decision Support System will enable users to apply backcasting methods to identify the sequences of CCAM measures that will result in their desired policy objectives.

1.2 Work Package 7 and Deliverable 7.3 within LEVITATE

This WP focuses on the impacts that the deployment of cooperative, connected and autonomous vehicles is expected to have on logistics and freight transport, through automated vans and trucks. Forecasting of impacts will consider these components: (i) Automation in parcel delivery, (ii) Automation in consolidation, (iii) Hub-to-hub automated transport, and (iv) the impact of platooning on bridges.
Forecasting will be based on the methodology developed in WP3 and the scenarios developed in WP4 to identify and test specific scenarios regarding the impacts of CCAM on freight transport. More specifically, the objectives of WP7 are:

- To identify how each area of impact (safety, mobility, environment, economy, and society) will be affected by CCAM in freight transport, with focus on the transition towards higher levels of automation.
- To test interactions of the examined impacts in freight transport scenarios; and,

- To create a policy support tool (PST) to help authorities to make the right decisions on policy measures concerning the introduction of CCAM.

The purpose of Deliverable 7.3 is to present the medium-term impacts of connected and automated driving in freight transport. The exact impacts of interest and how to measure these have been previously defined in WP3 and WP4. The specific nature of medium-term context has been defined in D7.1 (Hu et al., 2019). The main methodological approaches to forecast the medium-term impacts are simulation modelling and structural modelling . Simulation modelling will estimate the congestion on the road network-level impacts, while structural modelling will assess the impacts of truck platooning on bridges.

Table 1.1 shows an overview of the full list of impacts considered in the PST for WP7, along with a short description and the unit of measurement. Highlighted are those that are handled in this deliverable. Note that the list of medium-term impacts for other use cases urban transport (WP5) and passenger cars (WP6) is longer and further includes amount of travel (for person transport), modal split, shared mobility rate, vehicle utilisation rate and vehicle occupancy. However, these are not relevant for and not affected by freight transport. The amount of travel corresponds to the total freight kilometers, which is a short-term impact or direct impact for WP7 and has been covered in D7.2 (Hu et al., 2021).

Table 1.1: Overview of the impacts in WP7. Highlighted are the medium-term impacts for this deliverable.

Impact	Description / measurement	Unit of Measurement
Short term impacts / direct impacts		
Travel time	*Average duration of a 5Km trip inside the city centre*	*min*
Vehicle operating cost	*Direct outlays for operating a vehicle per kilometre of travel*	*€/km*
Freight transport cost	*Direct outlays for transporting a tonne of goods per kilometre of travel*	*€/tonne-km*
Medium term impacts / systemic impacts		
Congestion	*Average delays to traffic (seconds per vehicle-kilometer) as a result of high traffic volume*	*s/veh-km*
Truck platooning	*Impacts of truck platooning on highway bridges*	
Long term impacts / wider impacts		
Road safety	*Number of potential crashes per vehicle-kilometer driven (temp. until crash relation is defined).*	*crashes/ veh-km*
Parking space	*Required parking space in the city centre per person*	*m^2/person*
Energy efficiency	*Average rate (over the vehicle fleet) at which propulsion energy is converted to movement*	*%*
CO_2 due to vehicles	*Concentration of CO_2 pollutants as grams per vehicle-kilometer (due to road transport only)*	*t/day*
Public health	*Subjective rating of public health state, related to transport (10 points Likert scale)*	-
Road safety	*Number of potential crashes per vehicle-kilometer driven (temp. until crash relation is defined).*	*crashes/ veh-km*
Parking space	*Required parking space in the city centre per person*	*m^2/person*

2 Sub-use cases

A stakeholder reference group workshop (presented in detail in D7.1) was conducted to gather views on the future of CCAM and possible use cases of freight transport, termed sub-use cases (SUC), from city administrators and industry. A list of SUCs of interest for freight transport from the perspective of CCAM has been developed. Within LEVITATE, this list has been prioritized and refined within subsequent tasks in the project to inform the interventions and scenarios related to freight transport. In turn, these SUCs will be included in the LEVITATE Policy Support Tool (PST).

The prioritisation of the sub-use cases mainly took these three input directions into account:

- Scientific literature: Indicating the scientific knowledge and the available assessment methodologies for the sub-use cases. However, this might not be directly linked to their importance / relevance for practice.
- Roadmaps: Indicating the relevance of sub-use cases from the industrial/ political point of view, independent of available scientific methodologies.
- SRG Workshop: Containing first-hand feedback for the sub-use cases but might only reflect the opinions of organisations and people who participated.

The automated freight transport related sub-use cases that were formulated after this procedure are the following:

- **Automated urban delivery**: Future parcel delivery by automated vans and delivery robots.
- **Automated consolidation**: Extension of automated urban delivery by applying consolidation at city-hubs.
- **Hub-to-hub automated transport**: Effects of transfer hubs to facilitate automated trucks.
- **Platooning on urban highway bridges**: Impacts of increasing the density of heavy freight transport on bridge infrastructure and potential measures.

2.1 Automated urban delivery

The automated urban delivery sub-use case compares the performance of parcel delivery in urban areas via manual delivery personnel and (semi-)automated concepts. While the automated road-based (delivery) vehicles are well-studied, the operation of delivery robots or micro-vehicles is still an under-researched topic (Baum et al. 2019). Studies show that using smaller, electrified vehicles and robots addresses several acute problems: emissions, navigation in confined inner-city areas and the limitation of working time for manual parcel delivery (Jennings et al., 2019, Figliozzi et al., 2020). There are concepts where the autonomous delivery robots are airborne drones (Dorling et al. 2017), but the operation of drones especially in crowded urban environment is controversial and legally challenging. Therefore, this not further considered in the project.

Based on the current manual delivery process, the envisioned automation technologies and concepts that will emerge in the next decades, we consider these delivery scenarios:

- **Manual delivery** (status quo) is used as a base scenario for comparison.

- **Semi-automated delivery** assumes that the delivery process is not fully automated yet. While the delivery van is automated, personnel are still undertaking the delivery task. However, since they do not need to switch between delivery and driving tasks, time can be saved during each stop.
- **Automated delivery** is where so-called robo-vans and small autonomous delivery robots replace all service personnel and operate beyond the road (to the off-loading areas using pavement, pedestrian area, etc.). The automated van functions as a mobile hub where they perform short delivery trips to end-customers, i.e., a hub-and-spoke setup with moving hubs. The human-less delivery process can be carried out during off-peak hours when road traffic volumes are lower and be extended to evening or nighttime delivery. For this concept, we assume that the parcel capacity of the van will be significantly reduced. The main reason is that it has to carry the delivery robots and the necessary equipment to load them.
- **Automated night delivery** extends the previous scenario and applies night delivery only. This will result in an increase in fleet size since the total delivery has to be performed in fewer shifts.

The delivery performance and the limiting factors are shown in Table 2.1.

Table 2.1: Performance of the delivery scenarios and their main limiting factors (red).

Delivery scenarios	**Sub-use case specific scenarios (Automated urban delivery)**				
	Delivery scenario parameters				
	Delivery shifts	Avg. parcels per shift	Avg. parcels per stop	Service time per stop	Delivery vehicle
Manual delivery	6:30 – 15:00	150	Variable	5 min	Van
Semi-automated delivery	6:30 – 15:00	180	Variable	4 min	Automated van
Automated delivery	6:30 – 15:00, 18:00 – 24:00, 0:00 – 6:00	100	Variable	10 min	Robo-Van
Automated night delivery	18:00 – 24:00, 0:00 – 6:00	100	Variable	10 min	Robo-Van

2.2 Automated freight consolidation

The automated consolidation sub use case is a continuation of automated urban delivery. In this setting, the parcel delivery companies will consolidate their parcels at city-hubs instead of operating independently and delivering parcels straight to their final recipients. Ideally, the city-hubs and the last-mile delivery operate on a white-label basis, i.e., the delivery vehicles are not bound to a specific delivery company but operate the service for all companies. This removes a lot of redundancy in the delivery system nowadays. In addition, since these city hubs are closer to the city center than the original distribution centers, final delivery routes in a consolidated scenario are significantly shorter. This has a positive impact on the traffic and the environment (Allen et al. 2012, Quak et al. 2016). While the scientific works are more focused on finding the optimal locations for the hubs (Charisis et al. 2020), it is more of a political and urban planning problem in the real world.

We compare the following delivery scenarios:

- **Manual delivery** refers to the same scenario in the previous SUC

- **Automated delivery** refers to the automated delivery scenario in the previous SUC
- **Manual delivery with bundling at city hubs** uses bundled parcel delivery via city-hubs, but both the servicing of city-hubs and the delivery to end-customers are done manually.
- **Automated delivery with bundling at city hubs** is the final scenario that combines the automated delivery via robo-vans and the city-hubs for bundling.

In all automated scenarios, we assume that the delivery is done during day and night (c.f. automated urban delivery SUC), whereas the transport from distribution centers to city hubs is done during the night via automated trucks. Solutions or prototypes for automatic loading and unloading already exist for packages and pallets (Cramer et al. 2020).

2.3 Hub-to-hub automated transport

This sub-use case studies the impacts of AV truck terminals functioning as transfer hubs. The goal of these hubs is to facilitate the transition towards level 5 automation by supporting the operation of level 4 automated trucks that can operate on highways but not in urban environment. It is assumed that outbound freight containers from the city are passed to AV trucks at the terminal, which then take over the long-haul highway segment. At an AV truck terminal of the destination city, the container is passed to a manually operated truck again to bring it to the destination. An ideal location for such a terminal is at the city border with direct or good access to the highway. Figure 2.1 shows how this concept should work.
The main benefit of this approach enabled by AV truck terminal is that

- Long-haul freight transport is the most unappealing part for truck drivers, but the first thing that can be automated. Besides social benefits, the cost reduction is a significant factor. This concept supports the usage of AV trucks.
- For the urban highway, it is possible to reduce the usage during daytime and shift the freight transport towards night. This can be achieved by coordinating AV trucks to only depart during night hours.

A study by Berger (2016) shows that this concept is highly attractive for the long haul, where the driver wage takes one third of the total transport costs. It is also expected that the hub-to-hub connections will be dominated by autonomous trucks, while hub-to-delivery will be executed by hybrid and full-electric small to medium sized trucks (Novak, 2016).

For this SUC we consider a small area around a potential AV truck terminal including an urban highway segment with ramps. Two scenarios are compared:

- **Status quo** where manual container trucks are operating between their origin and destinations directly across the day.
- **Operation via transfer terminal:** During the day, manual trucks deliver their freight from origin to the AV truck terminal. During night, AV trucks ship the containers from the terminal to the destination terminals. Similarly, AV trucks from other terminals arrive across day and night, while the further transport into the city via manual trucks happen during the day.

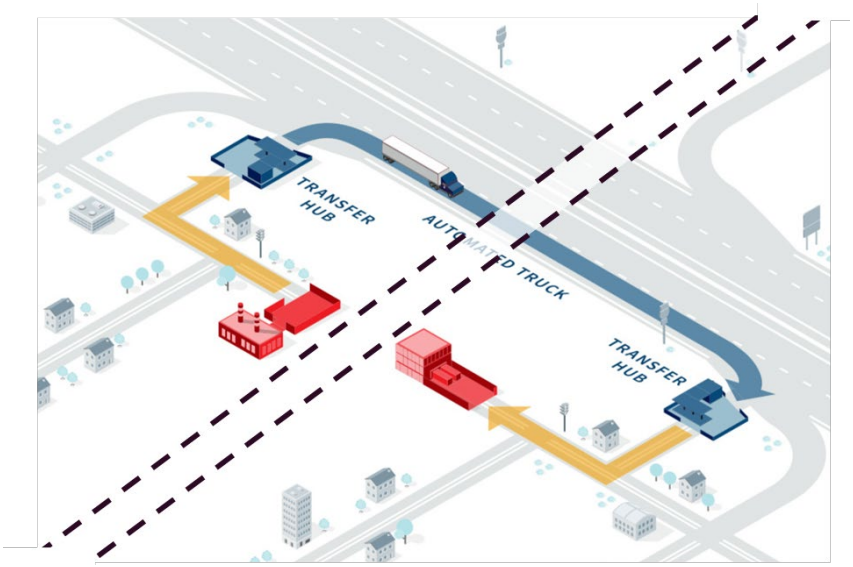

Figure 2.1: Function of the automated transfer hub. Human-operated trucks deliver the containers to the transfer hub (yellow arrow) and from there automated trucks carry them on to the highway (blue arrow).

2.4 Truck platooning on urban highway bridges

This sub-use analyses the potential effects of truck platooning on urban highway bridges. For truck platooning, there already exist a good amount of scientific work (Tsugawa et al. 2016, Humphreys et al. 2016), but the impacts on the bridge infrastructure is under-researched. The existing bridge stock was designed to carry traffic loads based on traffic composition at the time of creating the bridge-building codes. Truck platooning represents a change in the traffic composition, which has potential impacts on the bridge capacity to carry these new loads (Sayed et al. 2020). Following effects were identified as relevant and are analysed in this sub-use case:

- **Static traffic load effects**: the reduced vehicle distances in a platoon cause an increase of traffic load per road meter in the most used lane. Therefore, a potential increase of maximum traffic loads during bridge's lifetime can be expected.
- **Dynamic amplification**: the dynamic interaction between the vehicles, road surface and the bridge leads to an increase of the traffic loading. The repetitive composition of trucks in a platoon can potentially increase the values of dynamic amplification, if the interaction with bridge resonance properties turns out to be unfavourable.
- **Braking forces**: the total braking force of all vehicles on the bridge must be transferred from the bridge to the subgrade. Bridge bearings and/or piers assume this function. Trucks in a platoon are expected to brake in a coordinated way, which potentially increases the total braking force in comparison to flow of independent vehicles.

3 Methods

The types of impacts that are presented in Deliverable 3.1: A taxonomy of potential impacts of connected and automated vehicles at different levels of implementation (Elvik et al., 2019) have been estimated and forecasted using appropriate assessment methods, such as traffic microsimulation and operations research. Methods for the bridge modelling are presented more extensively since they are only applied to the platooning on urban highway bridges SUC. They include structural modelling and methods for calculating the traffic load effects. All these results relating to the relationships between sub-use cases, impacts and any intermediate parameters will be provided to WP8 of LEVITATE, which concerns the development of the LEVITATE Policy Support Tool (PST). The results will be integrated within the PST modules and functionalities so that impact assessment can be carried out by the users.

3.1 Microscopic simulation

We use the traffic micro-simulation framework AIMSUN next to assess the traffic impacts such as congestion and road safety. Compared to the SUCs in urban shuttles (WP5) and passenger cars (WP6), micro-simulation simulation has a lighter role in WP7 for these reasons:

- Freight vehicles only takes a small share of the traffic volume in urban areas and their impact is limited when compared to the overall traffic.
- Parameters of automated freight vehicles are still uncertain compared to automated passenger cars. Therefore, the results are less reliable.
- Freight operations are plannable; therefore, operations research is more suitable for the primary impacts such as fleet size and mileage.

Therefore, in this work package micro-simulation has the task to provide an estimation of traffic impacts in a small area (or for reference delivery tours), which serves as input for upscaling via operations research in the hybrid assessment approach.

3.1.1 Automated urban delivery and automated consolidation

For the automated delivery and automated consolidation SUCs, the simulation area is based on Vienna, an OSM import from the 19th district. For the calibration, we added traffic volume and traffic lights which mimic the real traffic conditions. The delivery tours are approx. 3km long and we use two settings:

- Route A mimics the periphery area by using low-traffic roads.
- Route B mimics the urban area by using more crowded roads.

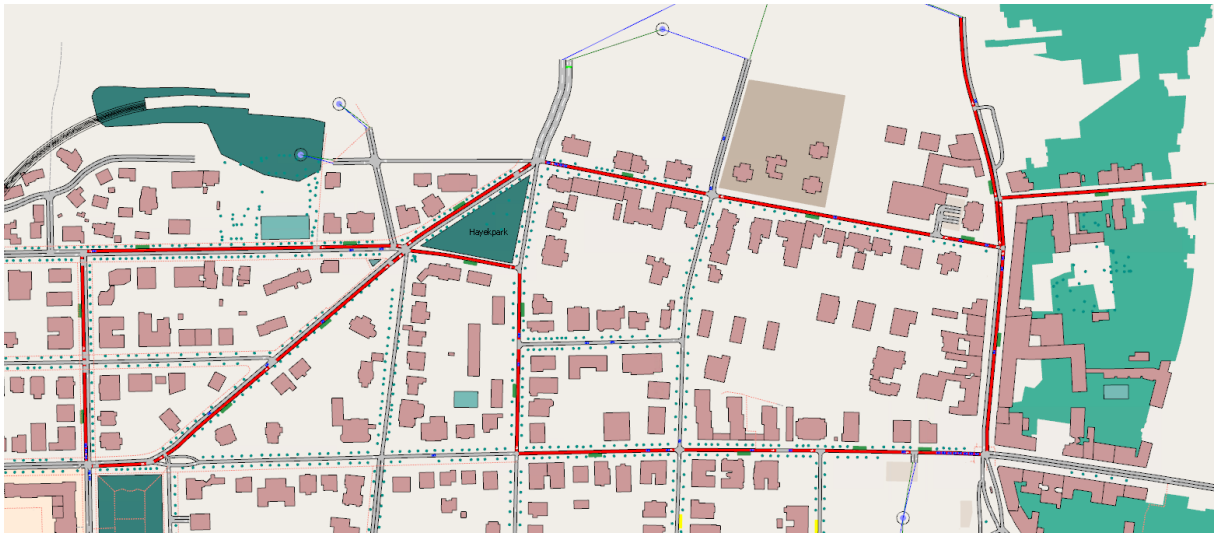

Figure 3.1: Simulated area for route A.

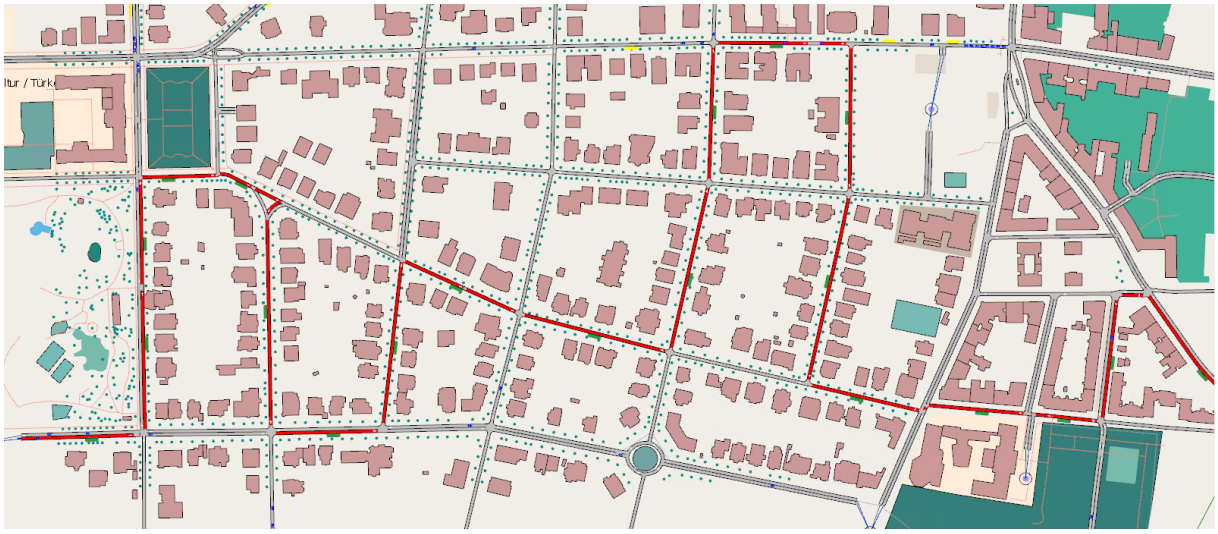

Figure 3.2: Simulated area for route B.

Scenarios

The delivery scenarios are listed in Table 3.1. The goal is to obtain results for the delivery scenarios that can be combined and upscaled for the hybrid assessment approach to reach the city level.

Table 3.1: List of delivery scenarios for the automated delivery and automated consolidation SUCs.

Delivery scenarios	**Automated urban delivery**		
	Simulation scenario parameters		
	Area	Delivery	Time
Set 1	urban	robo-van	day
Set 2	urban	manual van	day
Set 3	periphery	robo-van	day
Set 4	periphery	manual van	day
Set 5	urban	robo-van	night
Set 6	periphery	robo-van	night

The impacts of the delivery scenarios are influenced by the different autonomous vehicles penetration rate in the prevailing traffic. Regarding the implementation of connected automated vehicles (CAVs), different penetration rate scenarios were simulated and are presented in Table 3.2. The cautious CAVs, since they were considered to be the first generation, appeared first in the scenarios and then followed by the aggressive CAVs until the last scenario, where only 2nd generation CAVs were included. Both types are assumed to be fully automated vehicles with level 5 automation. The main idea behind modelling these two types is based on the assumption that technology will advance with time. Therefore, 2nd Gen CAVs will have improved sensing and cognitive capabilities, decision making, driver characteristics, and anticipation of incidents etc. In general, the main assumptions on CAVs characteristics are as follows:

- 1st Generation: limited sensing and cognitive ability, long gaps, earlier anticipation of lane changes than human-driven vehicles and longer time in give way situations.
- 2nd Generation: advanced sensing and cognitive ability, data fusion usage, confidence in taking decisions, small gaps, early anticipation of lane changes than human-driven vehicles and less time in give way situations.

The default car-following model in Aimsun Next is based on Gipps model (Gipps, 1981; Gipps,1986). Various parameters of the car-following model were adjusted to implement HDV and CAV behaviours. The assumptions on CAV parameters and their values were based on a comprehensive literature review, including both empirical and simulation-based studies (Cao et al.,2017, Eilbert et al.,2019; Goodall et al.,2020; de Souza et al.,2021; Shladover et al.,2012), as well as discussions in meetings with experts, conducted as part of LEVITATE project. Some guidance on the behaviours was also obtained through studies on ACC and CACC systems.

Note that we assume that the CAV penetration rate for freight vehicles to be different from passenger cars. The reason is that freight operators are economically driven. Once the technology is ready and offers a financial advantage, they will adopt faster. For passenger cars, adoption rate will be slower since subjective considerations (e.g., fun of driving a car) will influence the decisions.

In total, we run a simulation for every combination of delivery scenarios and CAV penetration rates, resulting in a total of 48 scenarios. In addition, for each scenario, 10 different replications with random seeds generating stochastic results were simulated as well for robustness of the results. The simulation duration of each scenario is 3 hours, and the simulation time step is set to 5 minutes.

Table 3.2: Scenarios for different CAV market penetration rates.

Type of Vehicle	A	B	C	D	E	F	G	H
Human-Driven Car	100%	80%	60%	40%	20%	0%	0%	0%
1st Generation (Cautious) CAV	0%	20%	40%	40%	40%	40%	20%	0%
2nd Generation (Aggressive) CAV	0%	0%	0%	20%	40%	60%	80%	100%
Human-driven freight vehicle	100%	80%	40%	0%	0%	0%	0%	0%
Freight CAV	0%	20%	60%	100%	100%	100%	100%	100%

Combination of delivery scenarios

As shown in Table 3.1, we obtain results for urban and periphery settings. Now we want to combine these results for each of the 23 districts in Vienna to approximate the "level of urbaness" best. For the sake of simplicity, we assume that each district has a certain share that matches the urban setting and a certain share that matches the periphery setting. Then the impacts of the micro-simulation are calculated as a linear combination of route A and route B for each district and added together to obtain the results on the city level:

$$impact\_of\ district\_i = impact\_route\_B * level\_of\_urbaness\_i + impact\_route\_A * (1 - level\_of\_urbaness\_i)$$

$$overall\_impact = \sum_{i=1\ldots23} impact\_of\ district\_i / 23$$

For estimating if a district is more urban than another, we use a metric based on the percentage of green areas, which are agriculture area, parks, forests, outdoor sport facilities and leisure areas. The lower the percental green area, the more urban is a district. A statistic in stadtbekannt[1] reveals the following data shown in Table 3.3. We assume the level of urbaness to be the inverted percentage of green area.

Table 3.3: Districts of Vienna and their level of urbaness.

District	Population	Green area	Level of urbaness	District	Population	Green area	Level of urbaness
1	16465	0%	**100%**	13	54171	70%	**30%**
2	105003	35%	**65%**	14	92337	60%	**40%**
3	90183	16%	**84%**	15	78999	9%	**91%**
4	33035	10%	**90%**	16	104323	31%	**69%**
5	55356	6%	**94%**	17	57180	53%	**47%**

[1] https://www.stadtbekannt.at/grnflchen-wiens/

6	31865	2%	**98%**	18	51128	27%	**73%**
7	32197	3%	**97%**	19	72107	48%	**52%**
8	25528	2%	**98%**	20	86868	8%	**92%**
9	42709	7%	**93%**	21	158712	41%	**59%**
10	198083	46%	**54%**	22	184188	56%	**44%**
11	100137	41%	**59%**	23	101053	31%	**69%**
12	95955	13%	**87%**				

3.1.2 Hub-to-hub automated transport

For the hub-to-hub automated transport SUC, the network is taken from a small area in the south of Vienna, which fulfils realistic conditions for the implementation of an automated transfer hub:

- Synergy: It is within an industrial area with a large number of logistic facilities, which provides the demand for the transfer hub.
- Accessibility: The location of the transfer hub is next to the highway ramp, which is essential for the operation of AV trucks at level 4 automation.
- Land acquisition: The considered area is unused and large enough, which facilitates the implementation at lower costs.

Figure 3.3 shows the location of the area within Vienna (left) and the envisioned location of the transfer hub (right). This area has been modelled into a simple model in AIMSUN shown in Figure 3.4. The traffic light circuits are modelled according to the real-world situation. The traffic volume is based on traffic counting on the highway, which reveals the daily inbound, outbound and thru traffic. To break down the traffic volume on an hourly basis, we take the time-dependent traffic volume for Vienna (Statistik Austria, 2020) as shown in Figure 3.5. We are aware that for an industry-heavy area the traffic distribution might be slightly different, but not essentially. In addition, especially the peak hours on the highway are accurate.

For the scenario where we assume that the automated transfer hub is implemented, we take the truck component of the overall traffic and modify the behaviour as follows.

- During the day (6am – 7pm), a proportion of trucks entering the highway via ramp are redirected towards the hub and return to their origin.
- During the night (7pm – 6am), the amount of automated trucks entering the highway corresponds to the amount of redirected trucks during the day.
- The inbound traffic is changed analogously, i.e., during the night, automated trucks arrive at the hub and during the day, the freight is picked up by the manual trucks.
- The proportion of redirected trucks correspond to the freight AV penetration rate (see Table 3.2).

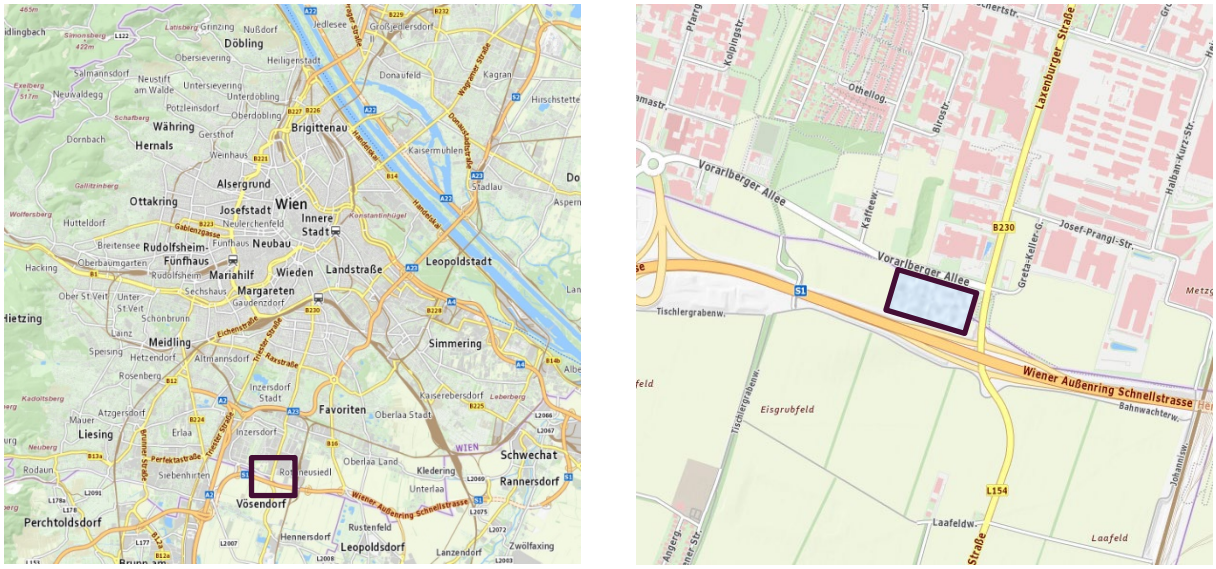

Figure 3.3: Area in the southern of Vienna where we assumed the location of the transfer hub.

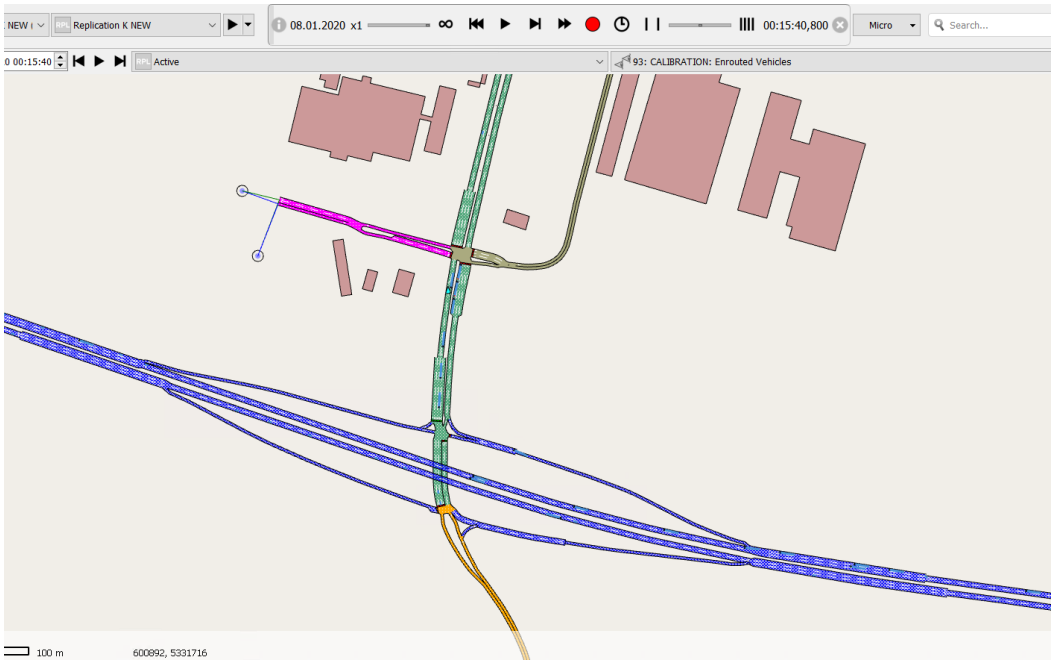

Figure 3.4: Modelled area for the transfer hub in AIMSUN.

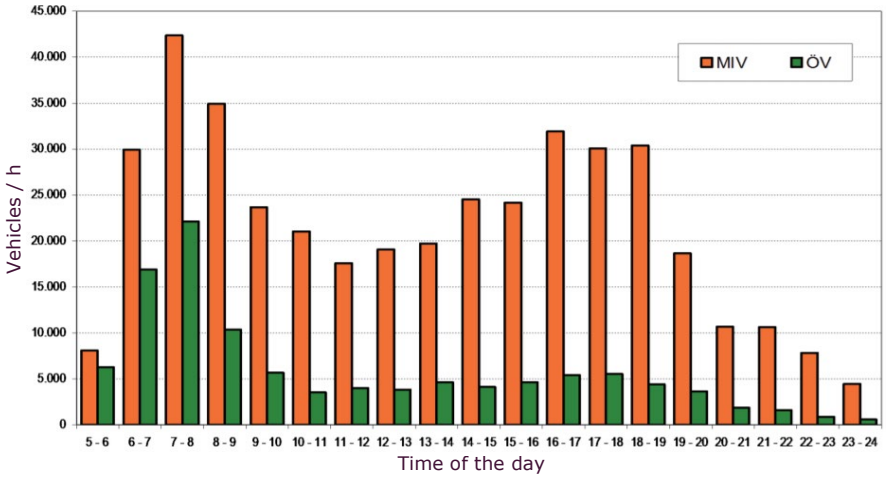

Figure 3.5: Time-dependent traffic volume in Vienna. No data are available from 0:00-5:00 because of the minimal traffic volume on the road. In the simulation this was set to half of the amount of 23:00-24:00.

3.2 Bridge modelling

This section describes the models and methods for the truck Platooning on urban highway bridges SUC. The model for traffic loads on bridges is standardized and defined in the EN-1991-2 (Eurocode[2]). It is representing the effects of vehicle loading and is manly used in the design of new bridges and with modifications in the assessment of the load bearing capacity of existing bridges (which are usually defined individually for each country respective to the bridge construction date). This traffic load model was derived based on axle-load measurements performed near Auxerre, France (Braml 2010, Sedlacek 2008) in 1986 and includes statistical assumptions for the future traffic volumes. The Eurocode 1 contains 4 different types of load models on road bridges. Most relevant is load model 1 (LM1), which is used for general and local verifications and was calibrated for loaded bridge spans of up to 200 m. Load models 2, 3 &4 cover the effects on short structural members, load of special vehicles and crowd loading of pedestrians. This work analyses the global ultimate limit states ULS (longitudinal bending moment and shear force), which are covered primarily by the load model LM1. EN 1991-2 allows a deviation from the defined load level LM1 by using adjustment factors α_{Qi}, α_{qi}, α_r which are defined in National Annexes to account for traffic compositions that differ from the basis traffic measurements used for deriving LM1.

To perform a site-specific calibration of traffic loads, it is necessary to know the traffic composition (vehicle types, their occurrence, their axle loads, etc.) and using this information to evaluate the expected maximum bridge loading during its lifetime. The actual traffic composition can be determined using Weigh-In-Motion (WIM) systems, which measure the axle loads in flowing traffic. To determine the expected maximum bridge loading, it is necessary to perform simulations that calculate the bridge loading caused by many years of simulated traffic. This approach was used here to compare the maxima of bridge loading in different traffic scenarios including also generic future load assumptions for truck platoons.

The following types of traffic scenarios were analysed:

[2] EN 1991-2: Eurocode 1: Actions on structures - Part 2: Traffic loads on bridges

- **Current heavy traffic** (status quo) used as a base scenario for comparison.
- **Heavy traffic with truck platoons:** different truck-platoons compositions mixed into the current traffic.
- **Intelligent access control:** heavy traffic with mixed-in truck platoons and imposed restrictions of minimum vehicle distances within platoons depending on carrying capacity of bridges.

3.2.1 Vertical traffic load effects on bridges

The traffic flow exerts different forces on the bridge, which must be transferred by the bridge structure into the subgrade. Usually the engineers divide the traffic forces on road bridges into vertical (weight of vehicles) and horizontal (braking, acceleration, centrifugal force) forces, which are also so defined in the different standardisations like EN 1991-2. Vertical forces dominate the action effects. They can be split into their quasi-static and their dynamic part. The quasi-static part represents the bridge-vehicle interaction without any inertia effects and is in principle equivalent to traffic load effects in case of an extremely slow travel speed ($v \to 0$). The dynamic part represents additional effects that arise from inertia and resonance effects of the interacting system bridge-vehicle, additionally influenced by road irregularities, at actual travel speed. If the Eurocode load models are used, all these aspects are already included in the defined load model. For the structural design at the ultimate limit state, additional load-side safety factors are included later. This is used for a semi probabilistic design procedure which is the most common approach.

Quasi-static traffic load effects on bridges are usually evaluated using influence lines / influence areas. The influence line is a function of axle load position on the bridge and describes the value of an internal bridge forces (e.g., the bending moment or shear force in a girder at point of interest) that would be produced by a unit axle force at different positions on the bridge. The total traffic-induced quasi-static cross-section force is then calculated as sum of influence line values at axle load positions (Figure 3.6) multiplied by the axle forces.

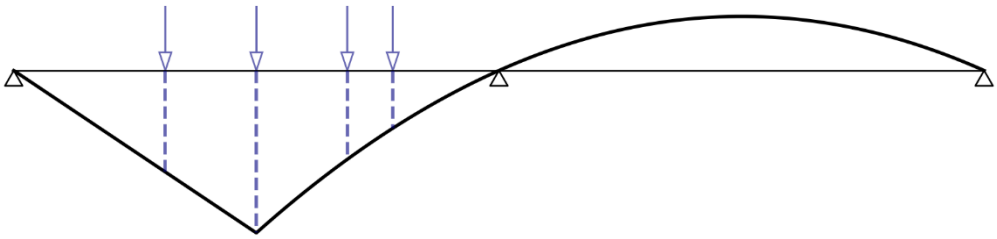

Figure 3.6: Scheme of an influence line for midspan bending moment of a two-span bridge, loaded with 4 axle forces.

Calculation can also be performed in a full probabilistic way, by using traffic-flow effects which includes synthesis of the time-history of traffic-induced cross-section forces (Figure 3.7 left). To evaluate the expected maximum load effect during bridge's lifetime in a probabilistic way, it is necessary to evaluate the cross-section force maxima in many equally long time periods and construct an extreme value distribution (Figure 3.7 right).

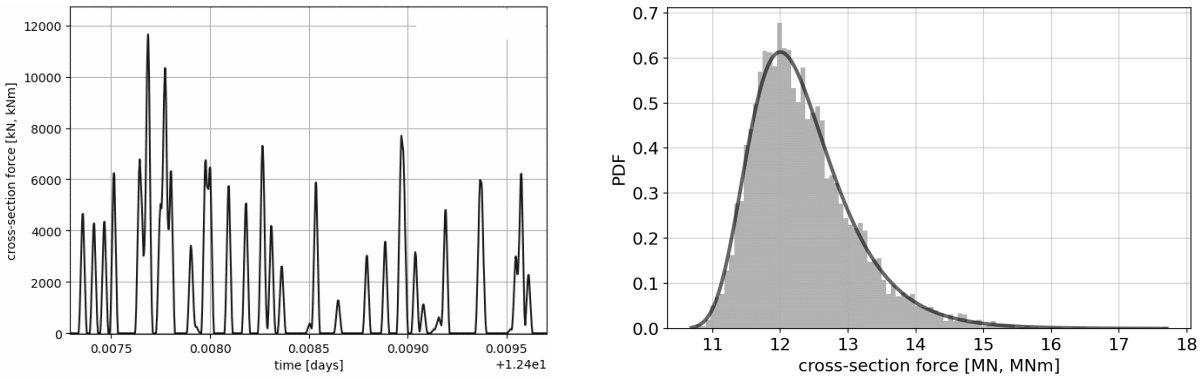

Figure 3.7: Example of time-history of bridge cross-section force (left); Example of histogram of weekly maxima with fitted extreme-value distribution (right).

Using the extreme value distribution, the probability of exceedance of different cross-section force levels can be evaluated. EN 1991-2 defines the characteristic value of load model LM1 by the exceedance probability of 5% in 50 years. It means that an 95%-quantile of the extreme-value distribution constructed using data of 50-years maxima is used as characteristic value for the design of new bridges.

The dynamic effect of traffic load actions increases the quasi-static cross-section forces. This increase, which is caused by traffic-induced vibrations of the bridge, is already included in the load model LM1 of Eurocode. However, when the load effects are synthesized from the traffic flow, the dynamic effects must be added to the quasi-static effects- which is usually done for railway bridges. An example of a comparison between quasi-static bridge response and the response including dynamic effects is shown in Figure 3.8. In this example, the maximum dynamic force is increased by 7% when compared to the quasi-static maximum.

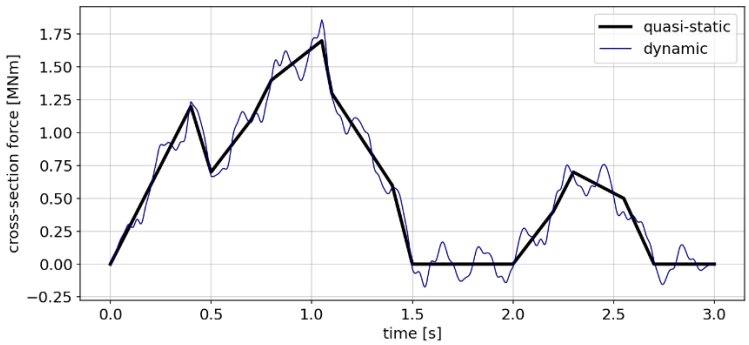

Figure 3.8: Comparison of quasi-static and dynamic history of the cross-section force (example).

3.2.2 Horizontal traffic load effects on bridges

EN 1991-2 prescribes the consideration of braking and acceleration forces, centrifugal forces, and lateral forces from skew braking and skidding. Among these forces, the braking force is the most relevant one in most cases. Therefore, this work will focus on the evaluation of braking forces only. Centrifugal forces occur on bridges with horizontal

curvature and will not be analysed here. Lateral forces from transversal braking and skidding are not relevant in standard cases and therefore will also not be analysed here.
The characteristic value of the braking force to be considered in the design of new bridges (Q_{lk}) is defined as:

$Q_{lk} = 0.6 \cdot \alpha_{Q1}(2Q_{1k}) + 0.1 \cdot \alpha_{q1} q_{1k} w_1 L$,

where α_{Q1}, α_{q1} are load-model adjustment factors with recommended value of 1,
Q_{1k} is the characteristic load of double axis in LM1; $Q_{1k} = 300kN$,
q_{1k} and w_1 are the uniform area load in the right lane and the lane width, respectively; with $q_{1k} = 9\ kN/m^2$ and $w_1 = 3\ m$ in most cases.

The force Q_{lk} should be placed as acting in middle of one lane.
Apart from the adjustment factors α, the interpretation of the above-mentioned formula is as follows:

- Scenario of vehicles braking in one lane needs to be considered.
- The primary braking force arises from 0.6g deceleration of an 60t truck.
- Additional braking forces arise from 0.1g deceleration of the remaining traffic flow in this lane, which can be assumed having a mass of 2.7 t/m in most cases.

Additionally, minimum and maximum values of Q_{lk} are given as:

$180\ kN \cdot \alpha_{Q1} \leq Q_{lk} \leq 900\ kN$

This model assumes a sequence of vehicles with different randomly distributed distances. Truck platooning represents a new, different scenario, where synchronized braking of trucks in the platoon occurs. Therefore, the braking forces of this new scenario will be analysed here and compared to braking forces of current traffic.

3.2.3 Assumptions

For the purposes of this work, following assumptions were made in the modelling of traffic flow, in the bridge assessment, and in the cost estimates:

Traffic flow on bridges

- Traffic flow is a random stationary process; evolution of the traffic flow over time is not considered.
- Vehicle speed is constant and all vehicles in one lane share the same speed.
- Vehicles do not change lanes while on the bridge.
- Most vehicles comply with the prescribed limits of gross vehicle weight. Vehicles that violate the prescribed limit do so in an appropriate manner – the excess weight is not very large. That means, a certain percentage of vehicles with gross weight slightly over 40 tons occurs, but for example a single vehicle with 60 tons does not (except for special vehicles that have the permit).
- Traffic composition and congestion properties according section 3.2.4
- The distribution of the number of vehicles between lanes is assumed as 80%-20% (Freundt et.al. 2011) for a two-lane urban highway in the case of low traffic intensity.
- Braking scenarios occur always in one lane only; the case that an obstacle spanning more than one lane occurs, is not considered, similarly to Eurocode.
- When a vehicle starts braking, the vehicles behind it start braking at the same time (driver reaction time is neglected).
- Each vehicle brakes with constant deceleration and the distance to previous vehicle at the end of braking maneuver is close to 0.
- First vehicle decelerates with $a_1 = 5.04\ m/s^2$

- Braking events occur approx. every 1000th vehicle.

Bridge assessment

- Bridges on the traffic route meet the current code requirements for positive assessment of existing bridges.
- Bridges behave as simply supported single span structures
- Simplified bridge models (beam model) are sufficient for purposes of this work

Cost estimates

Strengthening of bridge structures is considered as one option for dealing with potentially increased load-bearing demand. The cost of bridge strengthening is very difficult to estimate in general way. To give at least rough estimates of expected cost, following assumptions have been adopted (Figure 3.9). The cost estimates are expressed as the ratio of strengthening cost ($C_{retrofit}$) and bridge replacement cost ($C_{replacement}$). If the needed strengthening is not possible, then the bridge must be replaced, and the cost ratio is 1. The strengthening need is expressed as ratio of the design load (E_d) and bridge resistance (R_d). If the ratio $E_d/R_d < 1$, no strengthening is needed. A value of $E_d/R_d = 1.2$ means that 20% resistance increase is needed.

- Increase of bending moment resistance: Small retrofitting works (concrete layer, CFRP sheets) are expected to provide ~15% resistance increase and cost ~20% of a new bridge.
  Large retrofitting works (prestressing, girder strengthening) are expected to provide ~30% resistance increase and cost ~40% of a new bridge.
- Increase of shear force resistance: Small retrofitting works are expected to provide ~7% resistance increase and cost ~20% of a new bridge.
  Large retrofitting works are expected to provide ~15% resistance increase and cost ~40% of a new bridge.
- Increase of brake force resistance: Horizontal brake force is transmitted via bearings or piers, or both. Strengthening may include replacement of bearings, modification of abutments or pier strengthening. It is very difficult to provide reliable cost estimates. Therefore, cost estimates will not be attempted.

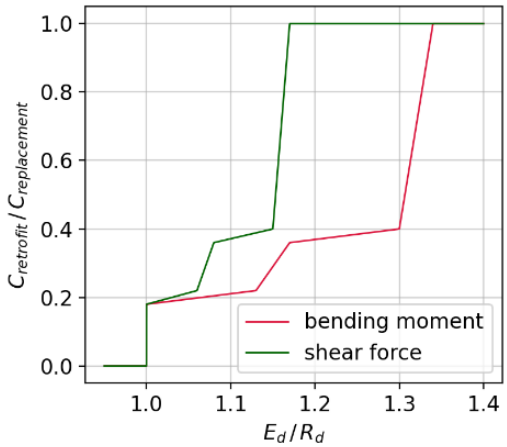

Figure 3.9: Assumed cost of bridge strengthening (rough estimates).

If bridge strengthening is needed, the limit states of bending moment and shear force are expected to determine the overall strengthening cost in the most cases and the cost estimates can be used as a first estimate in decision making.

3.2.4 Simulation of traffic flow on bridges

For the purposes of this work, a traffic model was adopted that was used for evaluation of traffic loads on bridges (Freundt et.al. 2011) and consecutively for adjustment of load models on bridges. This model synthesizes the traffic flow using the vehicle types listed in Table 3.4. It includes 5 truck types (one 2-axle truck type, two 4-axle and two 5-axle truck types), a crane and a personal car. The intended application of this model is the description of heavy traffic on intercity highways.

Table 3.4: Vehicle parameters – adopted from report of Freundt et al. 2011.

Vehicle type	Type 8	Type 33	Type 41	Type 97	Type 98	Crane	Personal car
Number of axles	2	4	5	4	5	6	2
	Axle distances [m]						
Axle 1-2	4.5	4.9	4.6	3.7	3.7	1.9	2.5
Axle 2-3		6.5	1.3	6.6	5.6	2.9	
Axle 3-4		5.0	5.2	1.3	1.3	1.7	
Axle 4-5			4.6		1.3	2.6	
Axle 5-6						1.7	
	Distribution of gross vehicle weight to individual axles						
Axle 1	44.9%	25.8%	20.9%	30.6%	20.8%	16.6%	50.0%
Axle 2	55.1%	37.2%	25.8%	30.9%	28.1%	16.6%	50.0%
Axle 3		18.9%	16.1%	19.1%	17.0%	16.6%	
Axle 4		18.1%	19.5%	19.4%	17.0%	16.6%	
Axle 5			17.7%		17.1%	16.6%	
Axle 6						16.6%	

The flowing traffic is further defined by:

- distances between vehicles, expressed as a probabilistic distribution,
- constitution of traffic in individual lanes – percentages of individual vehicle types in the whole traffic flow of each lane,
- gross vehicle weight, described by probabilistic distribution for each vehicle type,
- vehicle speed in each lane.

The distribution of gross vehicle weights is displayed in Figure 3.10. Passenger cars are modelled with a constant mass of 1 t and are of marginal relevance for the bridge loading. The distribution of truck weights is defined through joining of two normal distributions. Since normal distributions are unlimited, lower and upper limits of gross vehicle eights were additionally introduced. The distributions show a certain percentage of vehicles that violate the regulation of maximum permitted weight of 40 t (outliners). For vehicle types 41 and 98, almost 20% of the vehicles are expected to have gross weights over 40 tons. The crane is a special vehicle, where the 40t limit does not apply. These so-called special transports usually have to be approved in advance by the road operator.

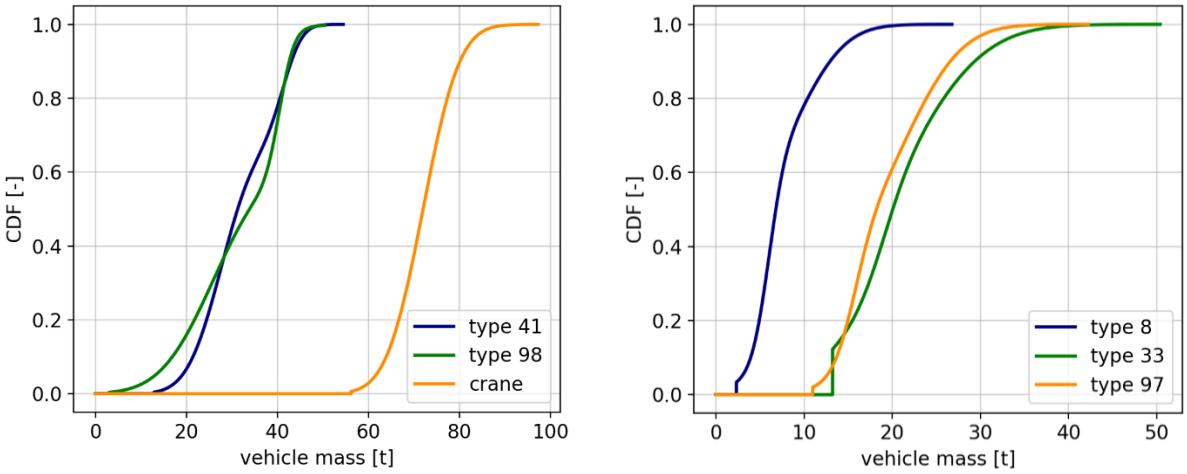

Figure 3.10: Distribution (Cumulative Density Function) of gross vehicle weight for different vehicle types according, with added lower and upper bounds.

The distribution of vehicle distances is dependent on the traffic intensity and is described by a lognorm distribution. The parameters of the distribution were adopted from (Freundt et.al. 2011) and are expressed by the expectation value (E_i) and standard deviation (σ_i) of the distribution for the i-th lane:

$$E_i = \frac{\overline{v_{fl,i}}}{n_{fl,i}} - \overline{L_{v,i}}\ ,$$

$$\sigma_i = 0.2967 \cdot E_i \cdot \left(n_{fl,i}\right)^{-0.6734}\ ,$$

where $\overline{v_{fl,i}}$ is the mean velocity [m/s] of flowing traffic of i-th lane, $n_{fl,i}$ is the number of vehicles per second [1/s] in the i-th lane, $\overline{L_{v,i}}$ is the mean vehicle length [m] in the i-th lane.

Since the distribution of vehicle distances describes the axle-distances (last axle of one vehicle to first axle of next vehicle), while the lognorm distribution starts at 0, it was necessary to modify this lognorm distribution in its bottom range, to prevent unreasonably short axle-axle vehicle distances. For this reason, samples of the lognorm distribution from the range 0 - 6.5 m were redistributed into the range 4 - 6.5 m (Figure 3.11), so that axle-distances below 4 m do not occur in flowing traffic.

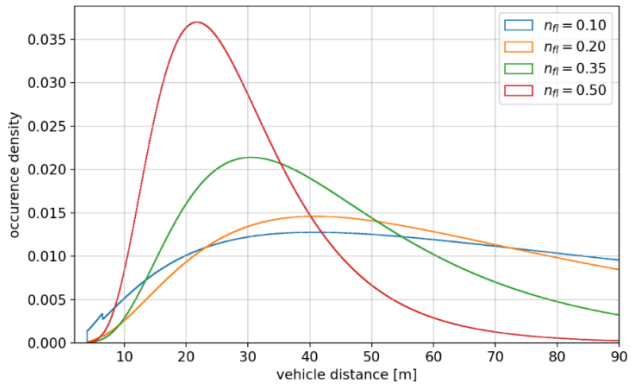

Figure 3.11: Example of vehicle-distance (axle-to-axle) distributions for traffic intensities from 0.1 to 0.5 vehicles/s with v_{fl}=80 km/h and L_v=15m.

The constitution of traffic is described by the ratios of vehicle numbers referring to particular vehicle types to total number of vehicles in a lane. Four different traffic constitutions (mixes) were simulated, which were adopted from (Freundt et.al. 2011) with slight modifications and are listed in Table 3.5. These traffic mixes are more typical for heavy intercity traffic; for example, there are no passenger cars in the right lane. The presence of a crane vehicle (gross mass 60~90 t) in traffic mixes B, C, D was restricted to the right lane to prevent its simultaneous occurrence in both lanes.

Table 3.5: Constitution of traffic, adopted with modifications (Freundt et.al. 2011).

Traffic mix	Lane	Vehicle						
		Type 8	Type 33	Type 41	Type 97	Type 98	Personal car	Crane
A	Right	11 %	5 %	17 %	8 %	59 %	0 %	0 %
	Left	2.20 %	1 %	3.40 %	1.60 %	11.80 %	80 %	0 %
B	Right	10.90 %	4.90 %	16.90 %	7.90 %	58.90 %	0 %	0.50 %
	Left	2.18 %	0.98 %	3.38 %	1.58 %	11.88 %	80 %	0 %
C	Right	10.90 %	4.90 %	16.90 %	7.90 %	58.90 %	0 %	0.50 %
	Left	4.19 %	1.89 %	6.50 %	3.04 %	22.84 %	61.54 %	0 %
D	Right	12.61 %	5.67 %	19.56 %	9.14 %	52.44 %	0 %	0.58 %
	Left	4.42 %	1.99 %	6.86 %	3.21 %	18.58 %	64.94 %	0 %

The distribution of the number of vehicles between lanes changes with the traffic intensity. The initial assumption for a two-lane highway (80% of vehicles drive in the right lane) starts to change using the implemented model when the mean time between vehicle passages drops below 1.5s (i.e., $n_{fl,i}$>0.667). Then, vehicles from the right lane start to redistribute into the left lane. Consequently, the traffic constitution in both lanes aligns as the traffic intensity increases. In this model, vehicles start to redistribute starting from traffic amount of ca. 50000 vehicles per day (in both lanes together). This causes reduction of time delay between vehicle passages in the left lane (Figure 3.12 left) and an increase of percentage of trucks in the left lane. Figure 3.12 right shows the composition of traffic in both lanes, where each color area represents the percentage of a vehicle type in the total number of vehicles in that lane.

To generate the traffic for bridge simulations, it is necessary to create samples of vehicle sequences using the given traffic parameters (composition of vehicles, traffic intensity, vehicle distance distribution, vehicle parameters). This is done by generating random samples of the given distributions, thus creating a random traffic flow that follows the given traffic parameters.

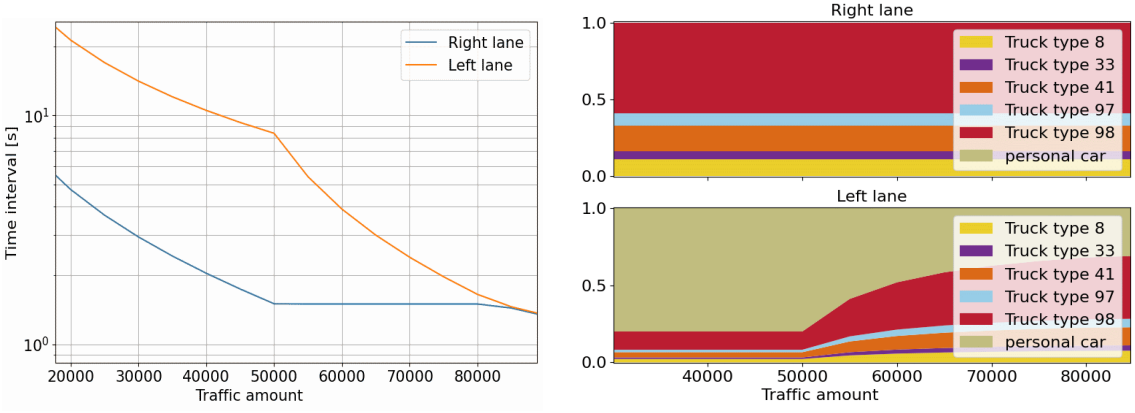

Figure 3.12: Change of traffic composition with increasing traffic amount. Mean time delay between vehicle passages (left); Composition of vehicle types in each lane (right).

Additionally, to flowing traffic, **congestion situations** need to be considered. The congestion is expected to produce traffic events that are most relevant for evaluation of maximum bridge cross-section forces, since more vehicle mass is concentrated on the bridge during congestions. A simple congestion model was adopted from (Freundt et.al. 2011), which is governed by two parameters:

P_{cong} is the probability that the following vehicle is congested, given that current vehicle is congested,

P_{flow} is the probability that the following vehicle is not congested, given that current vehicle is not congested.

Generation of congestion states of all vehicles in the right lane according these simple rules provides an estimate of congestion forming. Congestion in the left lane is modelled here as following the congestion states of the right lane.

Vehicle distances in congestion is an important parameter, which governs the concentration of mass on the bridge. Three models for vehicle distances were implemented. They are listed in Table 3.6 and describe distributions used for generating inter-vehicle axle distances in congestion, i.e., the distance from last axle of one vehicle to first axle of the following vehicle. Since the normal distribution is unbounded, additional limits were introduced, limiting the values of $\mathcal{N}(10{,}5)$ to the range 3~20 m.

Table 3.6: Inter-vehicle axle distances in congestion, adopted with modifications from (Freundt et.al. 2011)

Notation	Distribution	μ	σ	min.	max.
C_5	Constant	5 m	0 m	5 m	5 m
$\mathcal{U}(5{,}15)$	Uniform	10 m	2.89 m	5 m	15 m
$\mathcal{N}(10{,}5)$	Normal	10 m	5 m	3 m	20 m

The **braking scenario** implementation is described next. A simple braking model was implemented, where reaction time of the drivers is neglected, as well as vehicle distance reserve at the end of braking. This means that when the braking maneuver ends, the front of one vehicle almost touches the back of previous vehicle (Figure 3.13). All vehicles start braking at the same time and deceleration of each vehicle is constant.

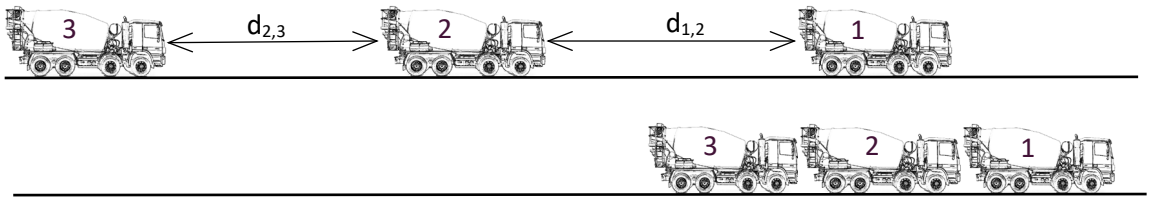

Figure 3.13: Scheme of braking scenario at start (top) and end (bottom) of the braking maneuver.

Given that all vehicles travel with the same velocity v, the distances between vehicles (from rear of one vehicle to front of next vehicle) at the start of braking are denoted as $d_{i,i+1}$ and the deceleration of vehicles as a_i, then the deceleration of the i[th] vehicle is for $i > 1$ given by:

$$a_i = -\frac{v^2}{2\left(\sum_{k=1}^{i-1} d_{k,k+1} + \frac{v^2}{2|a_1|}\right)}$$

The deceleration of the first vehicle (a_1) must be assumed. The definition of braking force in EN1991-2 suggests an assumed deceleration of 6 m/s². In this project, a value of $a_1 = 5.04\ m/s^2$ was used, which was adopted from the thesis of Kalakos and Westerhof 2017, as the experimental result from a braking test on dry asphalt in straight-line at 60 km/h.
The occurrence frequency of braking events must also be considered. Due to a lack of more detailed data, it was assumed that every 1000th vehicle starts a braking maneuver. In the actual software implementation, each vehicle was considered as starting the braking maneuver, and the results were treated as if acquired from a 1000-times longer time-period, which produces equivalent results.
To consider the most unfavourable case, the first vehicle in the braking maneuver starts braking at a position that introduces maximum braking force to the bridge: it stops at the end of the bridge. This maximizes the number of vehicles that are braking on the bridge. The total braking force of all vehicles that are braking on the bridge must be transferred via bridge bearings or bridge piers to the subgrade.
Table 3.7 shows three examples of braking force calculation using the above-mentioned methodology. The total braking force depends on gross mass of the vehicles and their distances. In the first example, three vehicles with short inter-vehicle distances are involved in braking, resulting in total braking force of 435.2 kN. Sum of vehicle lengths is 45 m, which means the vehicles could fit on a bridge with a 45 m span, upon which the total braking force would act.
The second example involves four vehicles with larger distances, leading to a total braking force of 449.3 kN. In both examples 1 and 2, the total braking force is below the value of the Eurocode-requirement, for which new bridges are designed.
The example 3 involves four heavy vehicles with very short distances. The total braking force amounts to 645.1 kN, which is already above the Eurocode-requirements. If this braking scenario would occur and the bridge bearings would not have additional force-transferring reserves beyond the Eurocode requirements, the bearings could be damaged, and the bridge superstructure could move from the bearings in an unforeseen manner. As mentioned above, the most unfavorable position of the braking vehicles was assumed here (first vehicle stops at the end of the bridge), to get conservative results.

Table 3.7: Three examples of braking force calculation results

Vehicle Nr.	Gross mass [t]	Length [m]	Distance to previous vehicle [m]	Deceleration [m/s²]	Brake force [kN]
Example 1					
1	40	15	-	5.04	201.6
2	25	15	8	4.33	108.3
3	35	15	12	3.58	125.3
	Length sum: 45 m			Sum of forces:	435.2 kN
Example 2					
1	30	19	-	5.04	151.2
2	40	15	15	3.86	154.3
3	35	15	30	2.63	91.9
4	25	15	25	2.08	51.9
	Length sum: 64 m			Sum of forces:	449.3 kN
Example 3					
1	45	15	-	5.04	226.8
2	40	15	6	4.49	179.6
3	35	15	8	3.92	137.2
4	30	15	10	3.38	101.5
	Length sum: 60 m			Sum of forces:	645.1 kN

3.2.5 Bridge response simulation

Since this sub-use case is intended to give a general analysis of the potential impact of truck platooning on urban bridges, it is sufficient to use simplified bridge models at this stage of analysis. In this simulation, simply-supported single-span bridges are considered. The bridge is modelled as a single beam supported at both ends, with free rotation.
The relevant limit states are the midspan bending moment and the shear force at the support(s). The traffic load effects are evaluated using the influence lines (Figure 3.14).

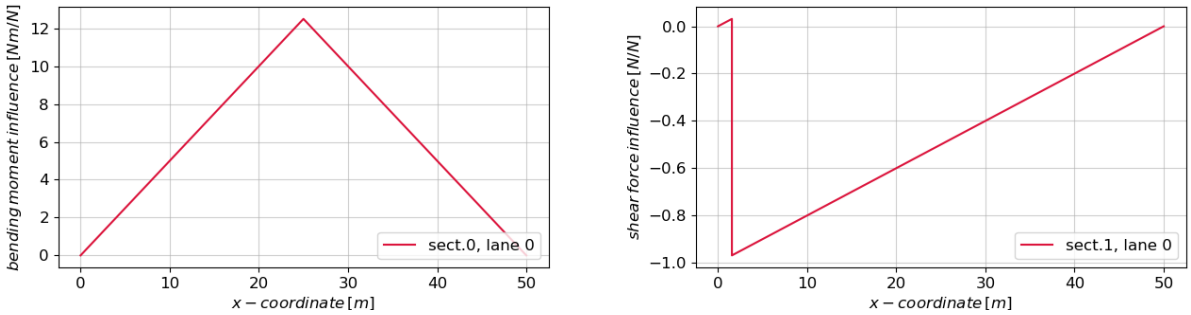

Figure 3.14: Example of influence lines of a simply-support single span beam with a span of 50 m. Influence on midspan bending moment (left) and shear force near the abutment (right).

Given the bridge models used here (simply-supported beam), the quasi-static traffic load effects are determined only by the bridge span; they do not depend on the type of bridge structure. On the other hand, the effects of permanent loads (bridge self-weight) depend very much on the bridge type. In this sub-use case, following bridge types were considered (the short notations are used in the remaining document):

- RCS: reinforced concrete slab,
- PCT: prestressed concrete T-beam bridge,
- PCB: prestressed concrete box-girder,
- CBG: composite bridge: steel girders + concrete slab,
- CBB: composite bridge: steel box-girders + concrete slab,
- SGO: steel bridge: steel girders with steel orthotropic deck,
- SBG: steel box-girder bridge.

a) RCS: Reinforced concrete slab

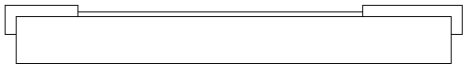

b) PCT: Prestressed concrete T-beam bridge

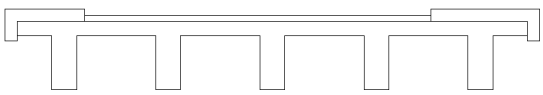

c) PCB: Prestressed concrete box-girder

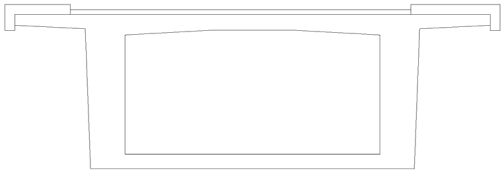

d) CBG: Composite bridge with steel girders

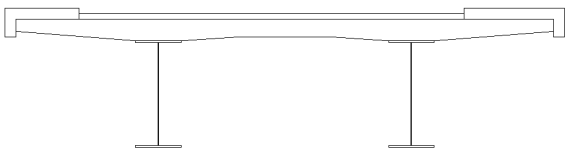

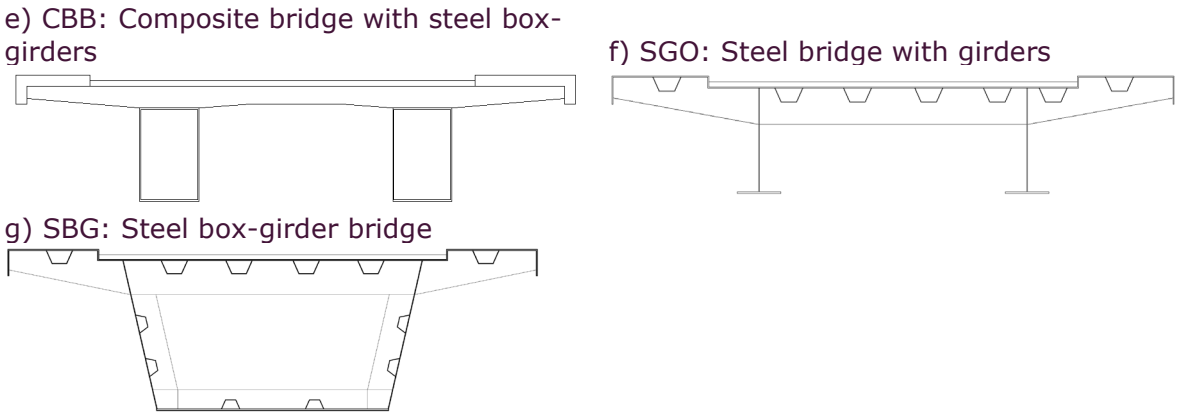

Figure 3.15: Cross-section schemes of the considered bridge types.

Given the simple bridge models used here, the consideration of different bridge types is reduced to the evaluation of the permanent load (self-weight). In all cases, apart from the self-weight of the load-bearing elements, additional permanent loads (road surface, edge beams) are considered with 300 kg per m² of the bridge surface. All bridges were modelled with a bridge deck width of 10.5 m (incl. edge beams), carrying two lanes. Table 3.8 shows the basic properties of the analysed bridge models. Besides bridge type and span length, the permanent load μ is listed, as well as the fundamental resonant frequency f_0.

Table 3.8: Basic properties of analysed bridge models

Type	Span [m]	μ [t/m]	f_0 [Hz]
RCS	15	29.4	5.65
RCS	15	22.8	4.17
RCS	20	38.2	4.30
RCS	20	29.4	3.18
PCT	20	16.8	5.83
PCT	20	14.9	3.77
PCT	25	19.2	4.78
PCT	25	16.7	3.17
PCT	30	21.6	4.04
PCT	30	18.4	2.72
PCT	35	24.0	3.49
PCT	35	20.1	2.38
PCT	40	26.4	3.07
PCT	40	21.9	2.10
PCB	40	21.1	3.20
PCB	50	23.7	2.57
PCB	60	26.8	2.12
PCB	70	30.4	1.80
PCB	90	37.1	1.38

Type	Span [m]	μ [t/m]	f_0 [Hz]
CBG	30	11.6	2.70
CBG	35	11.8	2.40
CBG	40	12.0	2.15
CBG	50	12.5	1.80
CBB	40	13.4	2.05
CBB	50	14.0	1.75
CBB	60	14.5	1.52
CBB	70	15.0	1.35
SGO	35	6.1	2.61
SGO	40	6.3	2.40
SGO	50	6.6	2.08
SGO	60	6.9	1.84
SBG	70	7.0	1.73
SBG	90	7.7	1.44
SBG	120	9.0	1.14
SBG	150	10.5	0.94

The quasi-static effect of traffic loads was evaluated using the influence lines. To evaluate the characteristic load, extreme-value distribution constructed from maximum values of 50-year time-periods should be used. Since it is not feasible to simulate many 50-year periods, shorter periods are used instead, and the result is converted. Given that the traffic is a stationary random process and the Gumbel distribution is used to describe the extreme

values, the resulting distribution can be converted to different reference periods by shifting the mean of the distribution. Figure 3.16 shows an example of shifting an extreme value distribution with reference time-period of 1 month (red) to reference periods of 1 year (green) and 50 years (blue). This approach allows to construct the extreme value distribution from 1-month maxima and convert it to expected 50-year maxima. For this purpose, 50 years of traffic flow is simulated, which allows to evaluate 600 monthly maxima, from which the extreme-value distribution of monthly maxima is evaluated and converted to expected 50-year maxima.

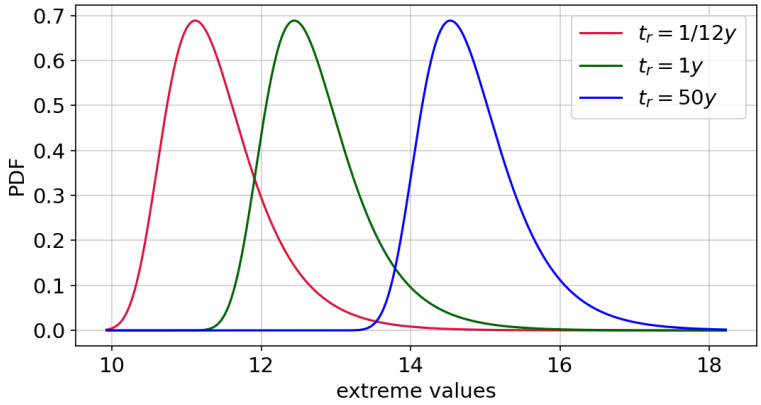

Figure 3.16: Scheme of shifting of extreme value distributions to longer reference periods.

To estimate the increase of cross-section forces due to dynamic effects incl. resonance, transient dynamic simulations were performed on simplified bridge models. Since it is not feasible to perform such calculations using the whole traffic flow, only a selected part of traffic events was analysed using dynamic calculations. From the simulated traffic flow in the period of 1 year, approx. 20000 traffic events were selected, which produced the largest quasi-static load effects. The dynamic amplification was then calculated for all these events using the moving-load model approach, where the secondary effects (vehicle dynamics and road evenness) are not taken into consideration to allow fast computation times. The dynamic effect was expressed in the form of the **D**ynamic **A**mplification **F**actor (DAF), which is defined as the ratio of max. dynamic effect and max. quasi-static effect (see also Figure 3.8). It is evaluated separately for each cross-section force of interest. The resulting DAF depends on the bridge structure and on the traffic loads. The simulation results showed the tendency to lower DAF-values for those traffic events that produce high cross-section forces in the bridge. This is a known effect, which results from random vehicle distances reducing the dynamic effects produced by individual vehicles. Figure 3.17 shows calculated DAF-values for two simulated bridges. The DAF-values of individual traffic events are shown as black dots, and quantiles of DAF (95%, 99%, maximum) in different bins (ranges) of quasi-static force are shown by green areas. $M_{q.st}$ and $V_{q.st}$ refer to the quasi-static bending moment and shear force maxima in simulated traffic events, while $M_{Q,k}$ and $V_{Q.k}$ refer to bending moment and shear force caused by the traffic load model LM1 of EN 1991-2. An already known trend of lower DAF values while higher loading (= increasing ratio of $M_{q.st}$ / $M_{Q,k}$) can be recognized.

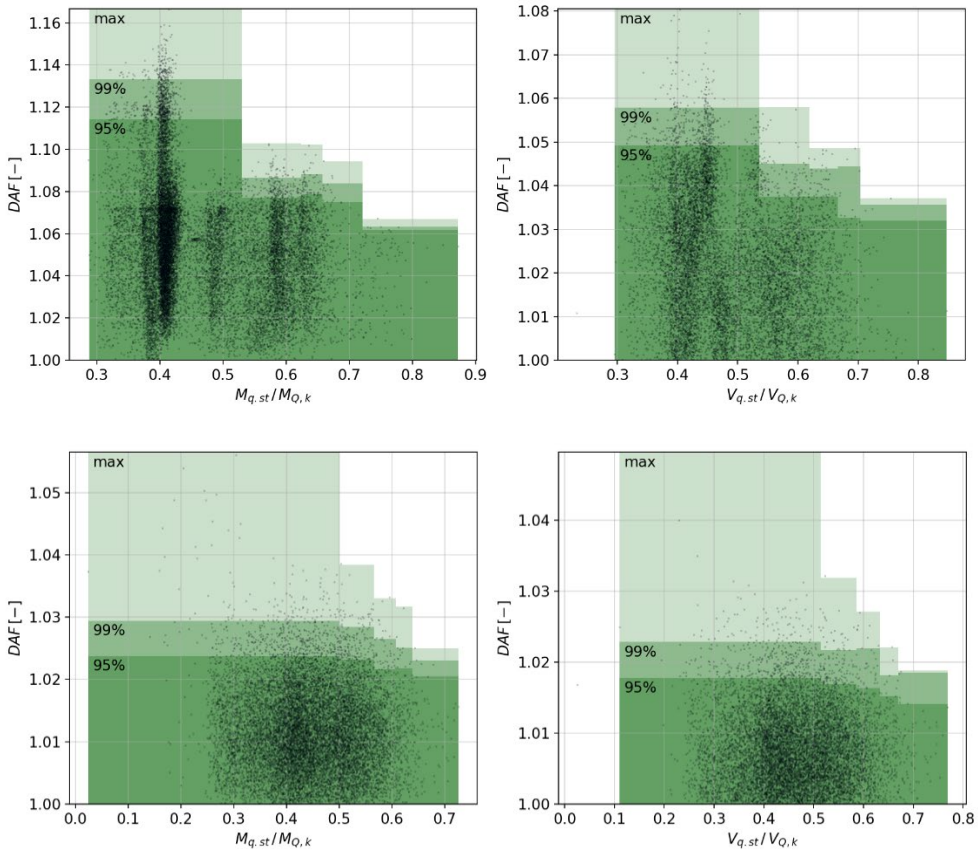

Figure 3.17: Calculated Dynamic Amplification Factors for different levels of bending moment (left) and shear force (right) in a prestressed-concrete T-beam bridge with 20 m span (top), and in a steel box-girder bridge with 90 m span (bottom).

Because the determining factor for bridge loading are extreme values, the DAF in the range of high quasi-static forces is relevant. Therefore, the 99%-quantile from the last bin (bin with highest ratio $M_{q.st}/M_{Q,k}$, $V_{q.st}/V_{Q,k}$) was used as the Dynamic Amplification Factor for current traffic loads and was evaluated separately for each analysed bridge model. Depending on the bridge, its values ranged from $DAF = 1.013$ to $DAF = 1.099$.

4 Obtained Impacts

4.1 Congestion

4.1.1 Automated urban delivery

For the automated urban delivery SUC, the results for congestion are shown in Table 4.1. Note that congestion is measured for the delivery vehicle, and not for the whole traffic in the background. The reason is that the background traffic would take a too high share compared to the single delivery vehicle and the effects would become negligible. This is different to WP5 and WP6 where congestion is measured for the whole traffic system. The columns show the simulation scenarios (c.f. Table 3.1) and the market penetration rates A-H (c.f. Table 3.2). The table is shown as a chart in Figure 4.1.

Table 4.1: Delay (s/km) for the delivery vehicles in the simulation scenarios. The values under the simulation scenarios are CAV market penetration rates (manual vehices, 1st generation AVs, 2nd generation AVs).

Simulation scenario	A	B	C	D	E	F	G	H
	(100,0,0)	(80,20,0)	(60,40,0)	(40,40,20)	(20,40,40)	(0,40,60)	(0,20,80)	(0,0,100)
urban, robo-van, day	45,6	49,0	46,5	39,1	52,4	42,1	38,7	46,1
urban, manual van, day	56,3	45,8	51,6	52,1	49,8	43,7	48,2	49,6
periphery, robo-van, day	26,0	25,8	25,7	25,5	26,0	25,9	25,5	25,3
periphery, manual van, day	28,6	29,2	29,5	31,5	32,2	31,9	29,7	31,2
urban, robo-van, night	4,3	4,4	3,1	4,2	4,2	4,0	3,4	4,0
periphery, robo-van, night	2,8	3,1	2,7	2,8	2,6	2,7	2,9	2,6

Note that the market penetration rates are for the general traffic, while the robo-vans are considered as changes in the logistics system. Therefore, scenario A (with AV penetration rate of 0%) with robo-vans is a theoretical combination which might not be relevant in practice. However, the impacts of this scenario are considered via simulation for the sake of completeness.

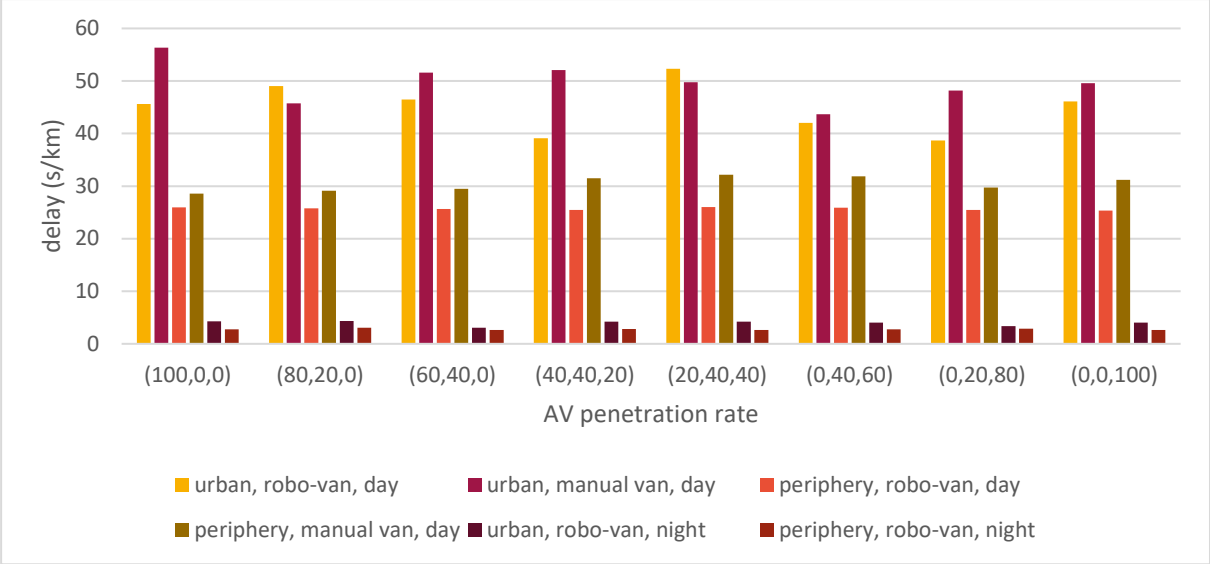

Figure 4.1: Delay (s/km) for the delivery vehicles in the simulation scenarios.

As mentioned in the last section "Combination of delivery scenarios", these results can be regarded as raw results and need to be combined to get a statement for the SUC. Therefore, for the automated delivery SUC, the congestion for every delivery scenario in every district is a combination of these simulation scenarios. The final results for the delivery scenarios are shown in Table 4.2 and Figure 4.2.

Table 4.2: Delay (s/km) for the delivery vehicles in the delivery scenarios.

Delivery scenario	A	B	C	D	E	F	G	H
	(100,0,0)	(80,20,0)	(60,40,0)	(40,40,20)	(20,40,40)	(0,40,60)	(0,20,80)	(0,0,100)
Manual delivery	48,9	41,3	45,7	46,6	45,1	40,5	43,3	44,7
Semi-autom. Delivery	40,4	42,8	40,9	35,5	45,3	37,7	35,2	40,5
Autom. Delivery	28,2	29,9	28,3	24,9	31,5	26,4	24,5	28,2
Autom. night delivery	3,9	4,0	3,0	3,9	3,8	3,7	3,2	3,6

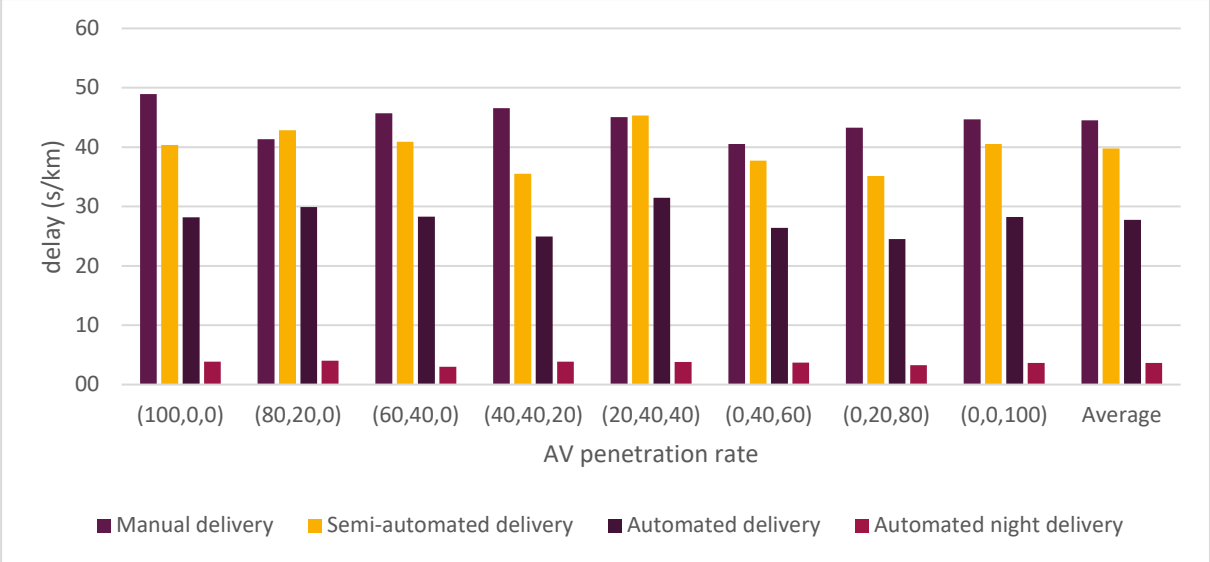

Figure 4.2: Delay (s/km) for the delivery vehicles in the delivery scenarios.

4.1.2 Automated consolidation

For the automated consolidation SUC, the baseline results are the same as for the automated delivery SUC, since the delay is stated as s/km for the delivery vehicles. With a delivery system using city-hubs, only the consolidation and the reduced mileage of the delivery vehicles are different. We recall D7.2 where we calculated the mileage of the different delivery scenarios with consolidation. Here we show them again in Table 4.3 to have an overview.

Table 4.3: Results for different delivery scenarios taken from D7.2.

	Delivery via van / robo-van					Bundle trips by trucks	
	#Tours	Fleet size	Ø Stops per tour	Ø Tour-length	Driven km	Driven km	Total driven km
Manual delivery	1799	1799	42,3	44,7 km	80389 km	-	80389 km
Automated delivery	2692	898	28,9	39,4 km	106177 km	-	106177 km
Manual delivery with city-hubs	1806	1806	17,8	13,7 km	24675 km	10445 km	35120 km
Automated delivery with city-hubs	2716	906	12,5	11,9 km	32347 km	10445 km	42792 km

Taking this numbers into account, we want to measure

a) the absolute delay caused to the delivery vehicles for each delivery scenario and
b) the delay caused to the traffic system by the delivery vehicles.

The absolute delay caused to the delivery vehicles is easy to calculate. If we neglect the different AV penetration rates and take the average delay multiplied with the mileage of the delivery vehicles for each delivery scenario, we obtain the total delay per day, see Table 4.4.

Table 4.4: Total delay for the delivery vehicles per day.

	#Tours	Fleet size	Driven km	Delay in s/km	**Total delay in h**
Manual delivery	1799	1799	80389 km	44,5	**993,8**
Automated delivery	2692	898	106177 km	27,7	**818,2**
Manual delivery with city-hubs	1806	1806	24675 km	44,5	**305,0**
Automated delivery with city-hubs	2716	906	32347 km	27,7	**249,3**

For b) the delay caused to the complete traffic system by the delivery vehicles, we analyse the simulation results with respect to the difference of delay in the background traffic, see Table 4.5. We observe that the difference between manual van and robo-van is less than +/- 2% in all scenarios, and statistically not significant. We conclude that the effects of the delivery vehicles on the whole traffic system is too marginal to be measured. Also, we note that the delay increases for scenario H, where only 2nd generation AV are in the overall traffic.

Table 4.5: Delay (s/km) for the background traffic in the simulation scenarios.

Simulation scenario	A	B	C	D	E	F	G	H
	(100,0,0)	(80,20,0)	(60,40,0)	(40,40,20)	(20,40,40)	(0,40,60)	(0,20,80)	(0,0,100)
urban, robo-van, day	19,2	18,6	18,7	18,6	18,4	18,3	18,5	19,2
urban, manual van, day	18,9	18,6	18,6	18,7	18,4	18,6	18,7	19,2
periphery, robo-van, day	9,5	9,1	9,4	9,1	8,9	9,0	9,0	9,2
periphery, manual van, day	9,2	9,2	9,3	9,0	9,0	8,7	8,9	9,3
urban, robo-van, night	1,3	1,1	1,2	1,2	1,2	1,2	1,2	1,2
periphery, robo-van, night	1,3	1,2	1,2	1,2	1,2	1,2	1,2	1,2

4.1.3 Hub-to-hub automated transport

Compared to the automated delivery and automated consolidation SUC, the simulated area for the hub-to-hub SUC only considers a small area around the transfer hub, as illustrated in section 3.1.2. Therefore, the effects of the transfer hub and the automation are more visible. The results in Table 4.7 and Figure 4.3 show the delay for both scenarios. Although the reduction is not very high when the transfer hub is used, it is visible, especially during the transition phase between scenario A (no AVs) and scenario H (full transition to 2nd generation AVs). In general, the simulated area is not very congested since it is in the border of Vienna and the large traffic volume is on the highway (with no traffic lights).

Table 4.6: Delay (s/km) for the background traffic with and without transfer hub.

Simulation scenario	A	B	C	D	E	F	G	H
	(100,0,0)	(80,20,0)	(60,40,0)	(40,40,20)	(20,40,40)	(0,40,60)	(0,20,80)	(0,0,100)
No transfer hub	9,7	8,8	8,6	8,0	7,8	7,5	7,4	7,3
With transfer hub	9,7	8,6	8,0	7,6	7,4	7,3	7,3	7,1

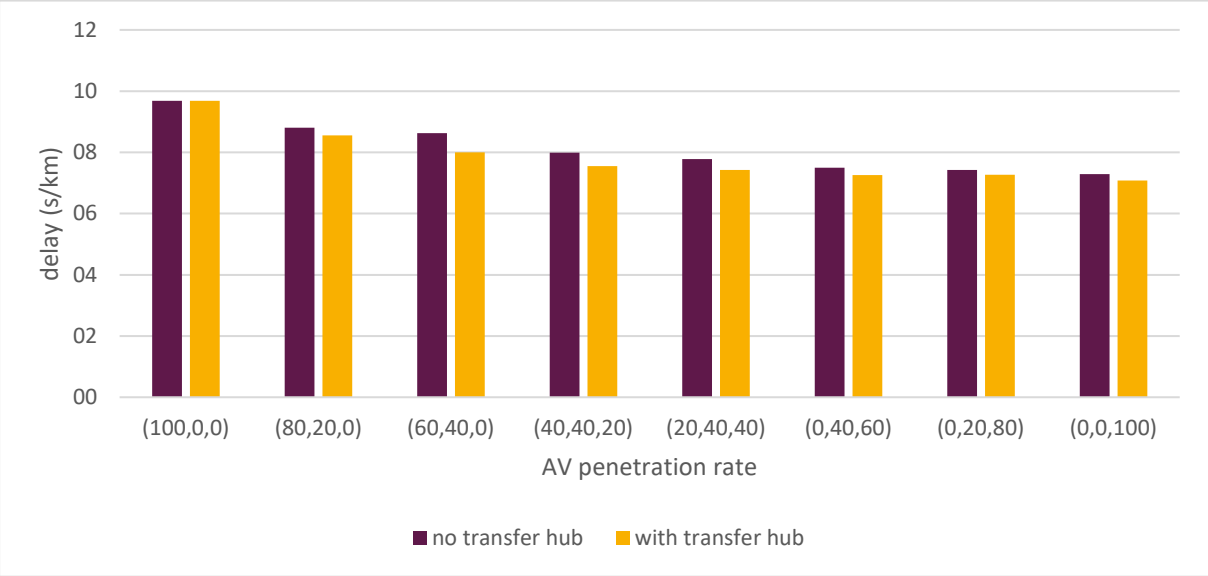

Figure 4.3: Delay (s/km) for the background traffic with and without transfer hub.

4.2 Platooning impacts on bridges

This section describes the impacts of platooning on bridges. The impact is threefold, and its description is divided into three subsections. The section 4.2.1 shows the impact in terms of reduction of structural safety of bridge structures. It describes the case when platooning would be introduced without additional measures (structural or traffic). Section 4.2.2 describes the case when the increased requirements on load-bearing capacity of bridges due to platooning would be solved through retrofitting of bridges. In this section, the retrofit needs are shown, and the costs are estimated. The section 4.2.3 describes the case when platooning is introduced with intelligent access control on bridges, to avoid overloading of bridges without bridge retrofitting.

4.2.1 No measures: reduction of structural safety

The change in traffic composition due to platoons is expected to lead to higher bridge internal forces, as described in section 3.2. The Ultimate Limit States (ULS) of midspan bending moment and shear force are analysed, as well as the horizontal force from braking. Their values in different traffic cases are compared. To make the results on different bridges comparable, the impacts are not expressed in absolute values of bridge internal forces, but relative to the bridge internal forces caused by Eurocode load model LM1. The forces caused by LM1 load model are deterministic, since the load model is deterministic. On the other hand, the simulated traffic is probabilistic, and the forces caused by this traffic are also evaluated as probabilistic, expressed through an extreme-value distribution (Figure 3.16). Therefore, the impact of simulated traffic is evaluated in terms of the probability of exceeding the effects of load model LM1. Since new bridges are designed for the loads of load model LM1, it is assumed that they have the respective load-carrying capacity. The definition of load model LM1 according to EN 1991-1 presumes that its exceedance probability in 50 years is 5%. Therefore, this probability (5% in 50 years) is regarded as the "code level". The resulting bridge forces are evaluated in terms of the probability, that they exceed the forces from Eurocode load models: bending moment $M_{Q,k}$, shear force $V_{Q,k}$, and the braking force $Q_{l,k}$. If the probability, that a resulting 50-years-extreme-value distribution exceeds the force from a Eurocode load model, is above 5% (i.e. $P\left(\max_{50y} M_Q > M_{Q,k}\right) > 0.05$, $P\left(\max_{50y} V_Q > V_{Q,k}\right) > 0.05$, or $P\left(\max_{50y} Q_l > Q_{l,k}\right) > 0.05$), the structural safety can be regarded as reduced. Higher exceedance probabilities mean lower structural safety.

Baseline scenarios

Baseline scenarios include all traffic cases without platooning. As expected, the traffic cases without congestions produced quite low bridge internal forces. Figure 4.4 shows the exceedance probabilities of the Eurocode LM1 effects for traffic mixes A, B, C, D, for the ULS of midspan bending moment of simply-supported single-span bridges of different span lengths ranging from 15 to 150 m.

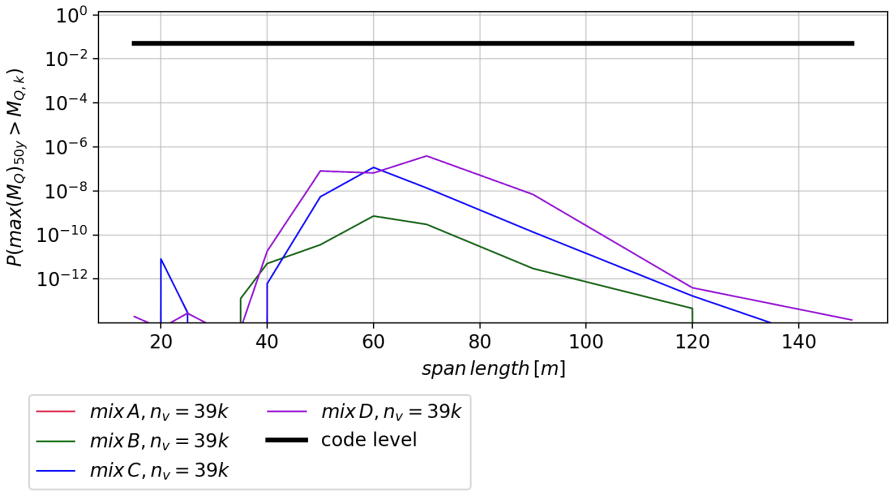

Figure 4.4: Bending moment exceedance probabilities for traffic without congestions and daily traffic volume of 39000 vehicles, for traffic mixes A, B, C and D.

Similar results were observed also for the ULS of shear force (Figure 4.5). The probabilities for traffic mix A were very low, so they do not appear in the figures.

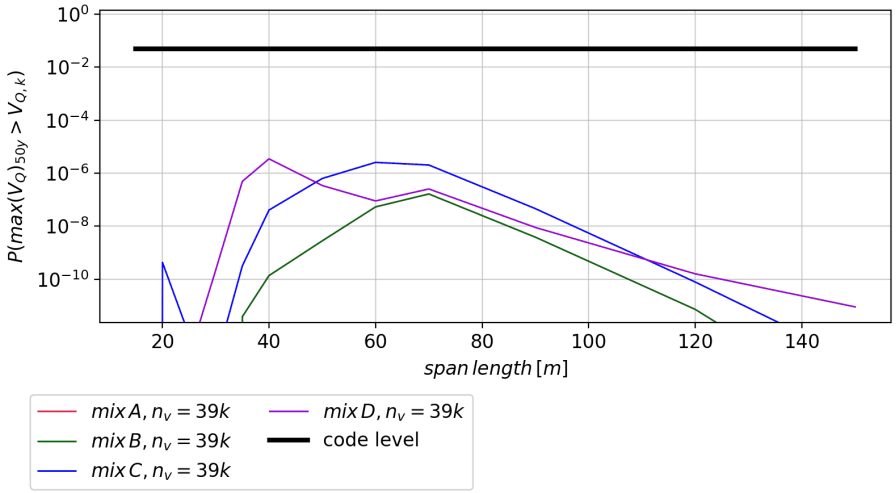

Figure 4.5: Shear force exceedance probabilities for traffic without congestions and daily traffic volume of 39000 vehicles, for traffic mixes A, B, C and D.

The traffic cases with traffic volume of 93000 vehicles per day produced similar results. The results presented above (95%-quantiles of extreme-value distributions with reference time period of 50 years) are well below the "code level" of 0.05 probability, primarily due to exclusion of congestions in traffic simulations.

The congestion events introduced a significant increase of bridge internal forces, especially on bridges with longer spans. Figure 4.6 shows the results for traffic with congestions (traffic cases 12, 13, 14) with different vehicle distances in congestion. Figure 4.7 shows similar results for the shear force. It is apparent that the congestions become more relevant for bridges with longer spans. The comparison of different vehicle distances in congestion suggests that the assumption of vehicle distances $\mathcal{N}(10,5)$ is more conservative

for bridges with span lengths up to 80 m for the bending moment ULS. For bridges with span above 80 m, the constant 5 m vehicle distance (C_5) is more conservative.
For the shear force ULS, the constant 5 m vehicle distance (C_5) produces more conservative results for almost all bridge span lengths.

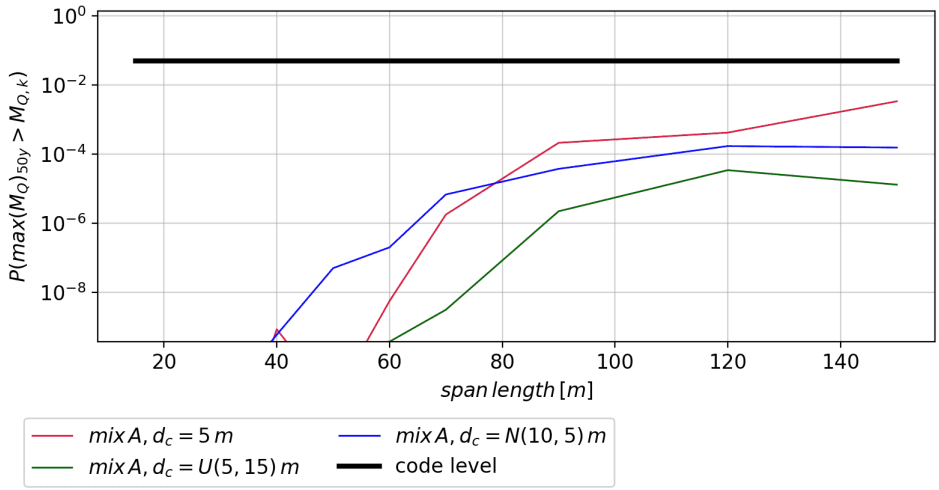

Figure 4.6: Bending moment exceedance probabilities for traffic mix A with different vehicle distances in congestion.

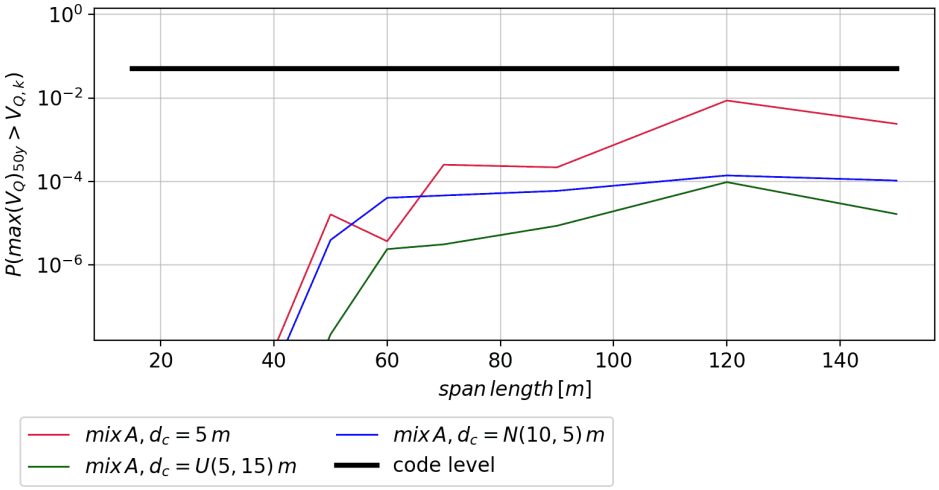

Figure 4.7: Shear force exceedance probabilities for traffic mix A with different vehicle distances in congestion.

The results from simulated traffic that includes congestions were still below the "code level" of 5% probability of exceedance in 50 years.

The simulation of braking scenarios produced braking force results that were larger than originally expected. Except for short bridges (L ≤ 25m), the calculated braking force maxima exceeded the values required by the Eurocode. The calculated braking force maxima occurred in cases where several successive heavy trucks were passing the bridge and the first truck started a braking manoeuvre. A truck with gross weight of 40 t produces during a full brake a force of ~200 kN. The consecutive trucks produce lower braking forces, depending on the distance to previous truck. In case of low vehicle distances and simultaneous presence of several trucks on the bridge, the sum of braking forces can easily

exceed the values required by the Eurocode (see also the example presented in Table 3.7). Due to the assumed constitution of traffic (large portion of trucks), this was often the case, and the total braking force in simulated braking scenarios exceeded the "EuroCode" values often at bridges of 30 m length and more.

Figure 4.8 shows the resulting total braking forces on bridges with different lengths between 15 m and 150 m. Shown are the 95%-quantile values of the 50-years extreme-value distributions. It can be observed that the expected braking force maxima depend on the bridge length and also on the traffic intensity. Higher traffic intensities lead to lower vehicle distances, and consequently to higher forces in braking events.

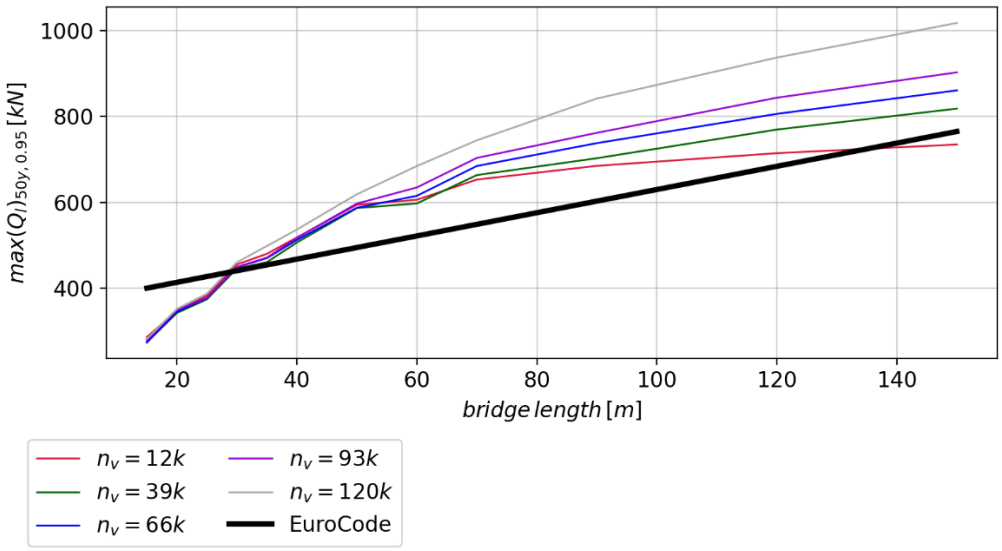

Figure 4.8: Braking forces: 95%-quantiles of extreme-value-distribution with reference time period of 50 years. Traffic mix A with traffic volumes of 12000, 39000, 66000, 93000 and 120000 vehicles/day.

In traffic mixes B, C, D, which include the crane vehicle, higher braking forces occur, due to the high gross vehicle mass of the crane and unchanged braking deceleration of $a_1 = 5.04\ m/s^2$. The results are shown in Figure 4.9. These results may be too conservative, if lower deceleration should be assumed for braking of the crane vehicle due to usually given restrictions given by the approvals of special (like lower limits of velocity, no additional traffic etc...)

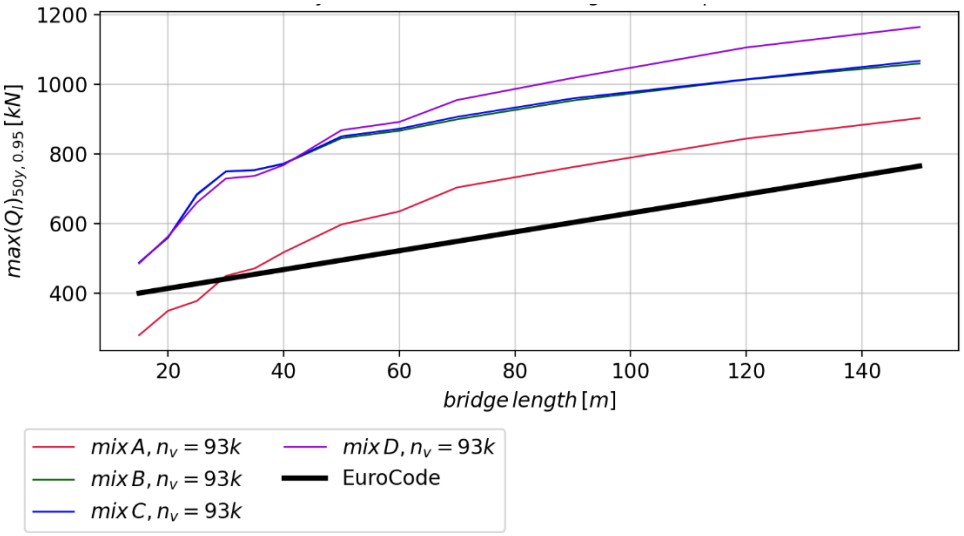

Figure 4.9: Braking forces: 95%-quantiles of extreme-value-distribution with reference time period of 50 years. Traffic mixes A, B, C, D with a traffic volume of 93000 vehicles/day.

Platooning scenarios

After the platoons were introduced into to the simulated traffic, the bridge internal forces increased significantly in bridges with longer spans. Figure 4.10 shows the increase of probabilities of exceeding the load effects of LM1 load model. The red curve is the traffic case with platooning (baseline), and four curves representing results with 20%, 40%, 60% and 80% platooning penetration rate are shown.

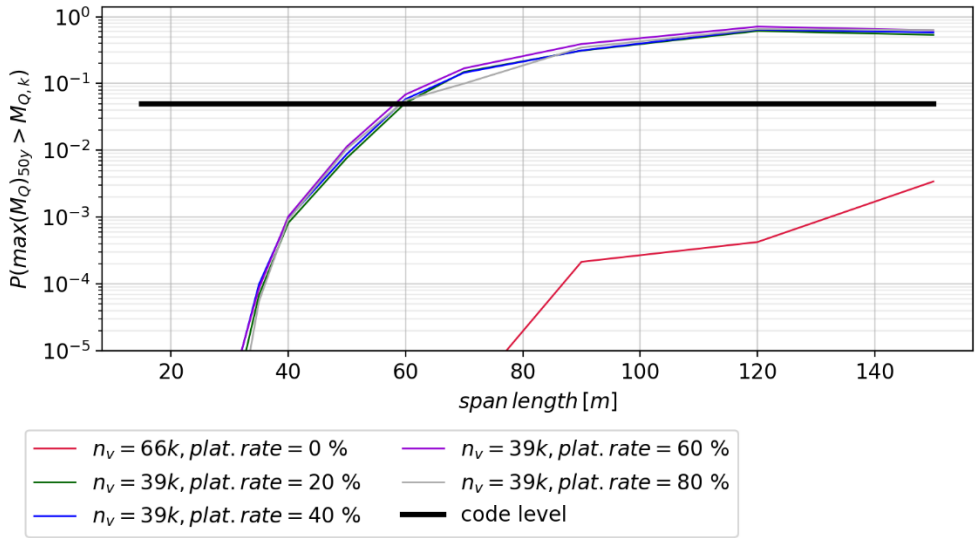

Figure 4.10: Bending moment exceedance probabilities for traffic mix A, constant congestion distances (C_5), P_{cong}=0.99, P_{flow}=0.999, traffic volume of 39000 vehicles/day and different platooning penetration rates.

It can be observed that the platooning penetration rate does not have significant effect on the exceedance probabilities. Even a low penetration rate of 20% produced already a large increase of exceedance probabilities.

Figure 4.10 presents results for the bending moment ULS. The results for the shear force ULS are very similar (Figure 4.11).

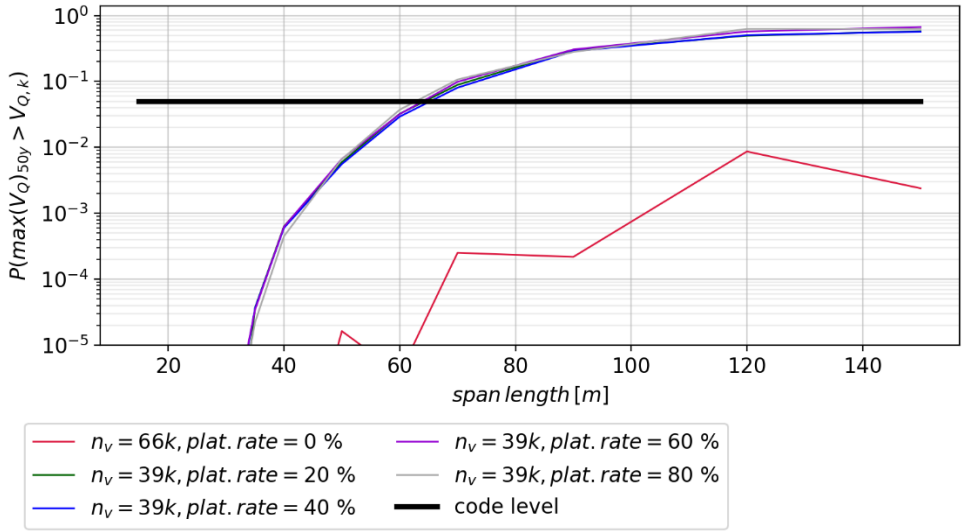

Figure 4.11: Shear force exceedance probabilities for traffic mix A, constant congestion distances (C_5), P_{cong}=0.99, P_{flow}=0.999, traffic volume of 39000 vehicles/day and different platooning penetration rates.

The results presented above indicate that starting from bridge span length of 60 m, the "code level" of exceedance probabilities is exceeded. Consequently, the structural safety of the affected bridges would be compromised, assuming that their load-carrying capacity is on par with the EuroCode requirements, i.e. without additional reserves.

To investigate the effect of congestion properties, which had to be assumed, their values were varied. Figure 4.12 shows the effect of different congestion assumptions. The difference between congestion distance models (C_5 vs. $\mathcal{N}(10,5)$) was not significant. The difference in congestion probabilities ($P_{cong} = 0.99$ & $P_{flow} = 0.999$ vs. $P_{cong} = 0.999$ & $P_{flow} = 0.9999$) produced an observable effect in the resulting exceedance probabilities. Since higher values of P_{cong} lead to more contiguous congestions, the effect can be observed in slightly higher exceedance probabilities for the case with $P_{cong} = 0.999$ compared to the case with $P_{cong} = 0.99$.
Figure 4.12 shows the effect on bending moment ULS; the results for the shear force ULS were very similar.

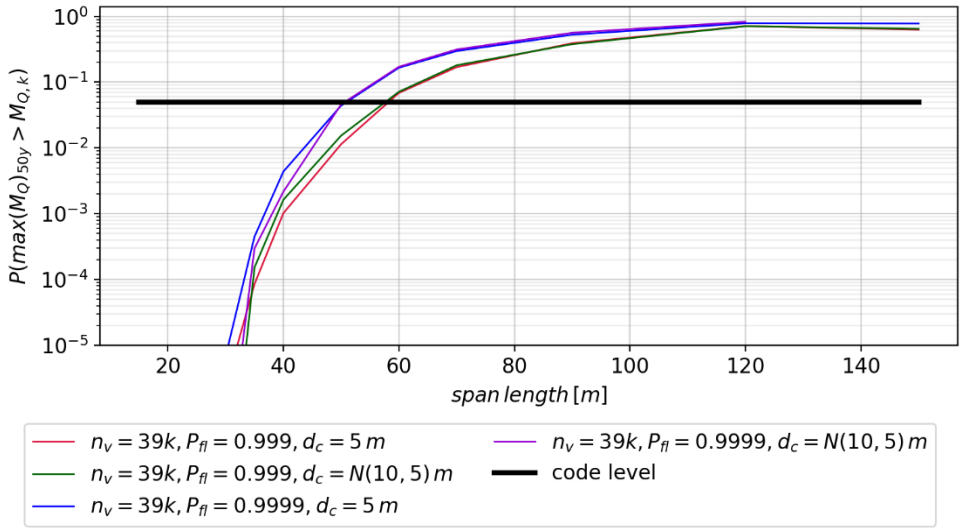

Figure 4.12: Bending moment exceedance probabilities for traffic mix A, traffic volume of 39000 vehicles/day, platooning penetration rate 60% and different congestion parameters.

The largest effect of platooning was observed for the criteria of braking forces. The extremely short distances within a platoon and the sequence of truck platoons lead to high forces in case of braking. This is because the trucks in a platoon need to brake with almost the same deceleration, so that all platoon vehicles decelerate with approx. 5 m/s². Additionally, more trucks fit on the bridge at the start of braking compared to the case without platoons. The effect becomes even more apparent for larger bridge lengths. Figure 4.13 shows the effects, where the red curve represents the baseline without platooning and four curves representing different platooning penetration rates are shown (they overlap into only one visible curve). For bridges above 80 m length, the braking force is at least the double of the baseline scenario.

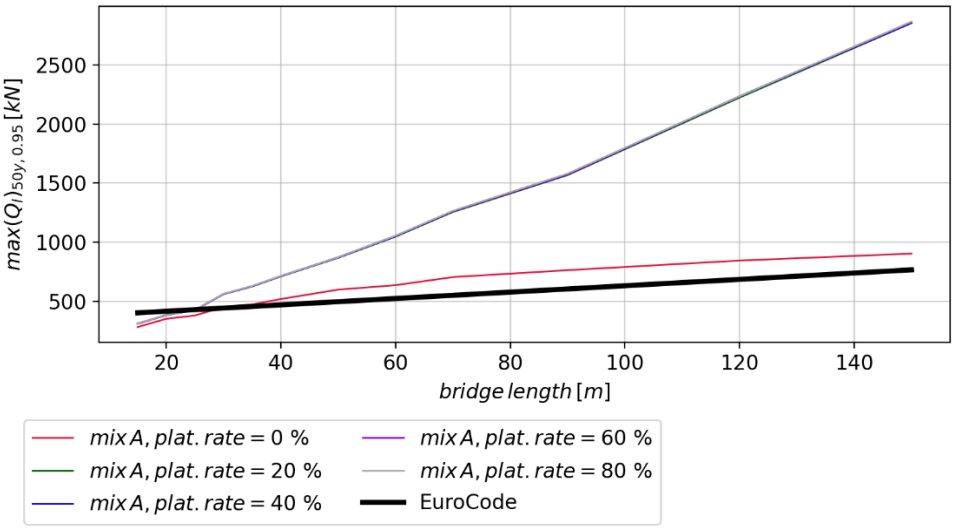

Figure 4.13: Braking forces: 95%-quantiles of extreme-value-distribution with reference time period of 50 years. Traffic mix A with different platooning penetration rates.

4.2.2 Bridge strengthening

The previous chapter presented the simulation results in the form of exceedance probabilities of the traffic load effect of the LM1 load model. In case of platooning scenarios, the new traffic load effects exceeded the effects of load model LM1, for which new bridges are designed, at bridges with larger spans.

One solution to avoid insufficient structural safety in light of new traffic scenarios would be the strengthening of the affected bridges. This means that structural retrofitting would be performed to increase the load-carrying capacity of the affected bridges. Depending on the level of required strengthening, the retrofitting works may include smaller measures such as new concrete layer or glued CFRP strips, or larger works such as additional prestressing or strengthening of girders.

In order to provide rough estimates of strengthening needs, it is necessary to express the them in the form of the ratio of required bridge resistance to present bridge resistance. In this step, the permanent loads (self-weight of all structural and non-structural elements of the bridge) must also be considered. The total load that acts on the bridge consists of permanent loads and traffic loads. Other loads (e.g. temperature) can be neglected for the purposes of this project. One important parameter for planning of bridge strengthening is required increase of resistance expressed in percent of the current resistance:

$$\Delta R_{req} = \frac{E_{new} - R_0}{R_0} \cdot 100\%$$

where ΔR_{req} is the required increase of resistance,
E_{new} are the total bridge load effects that consider the new traffic scenario,
R_0 is the current bridge resistance.

The current bridge resistance varies individually from structure to structure; some bridges have structural reserves that go beyond the code requirements, other existing bridges do not fulfil current requirements for new design. The EuroCode recommends the use of load model LM1 in assessment of existing bridges, but allows its reduction using the α_Q factors to account for less demanding traffic compositions. Therefore, some national or regional regulations use factors $\alpha_Q < 1$ in assessment of existing bridges.
Assuming that existing bridges fulfil the requirements on their positive assessment, three cases of bridge resistance levels are considered:

- $\alpha_Q = 1$: Bridge is able to carry exactly 100% of the LM1 load model
- $\alpha_Q = 0.9$: Bridge is able to carry exactly 90% of LM1 load model
- $\alpha_Q = 0.8$: Bridge is able to carry exactly 80% of LM1 load model

Further, following notations will be used:

$M_{g,k}, V_{g,k}$ – bending moment and shear force due to characteristic permanent loads,
M_q, V_q – bending moment and shear force due to LM1 load model,
M_{qnew}, V_{qnew} – bending moment and shear force due to new traffic scenarios.

Therefore, the required increase of bending moment resistance ($\Delta R_{M,req}$) and shear force resistance ($\Delta R_{V,req}$) was evaluated as follows:

$$\Delta R_{M,req} = \frac{(M_{g,k} + M_{qnew}) - (M_{g,k} + \alpha_Q \cdot M_{q,k})}{M_{g,k} + \alpha_Q \cdot M_{q,k}} = \frac{M_{qnew} - \alpha_Q \cdot M_{q,k}}{M_{g,k} + \alpha_Q \cdot M_{q,k}} \cdot 100\%$$

$$\Delta R_{V,req} = \frac{V_{qnew} - \alpha_Q \cdot V_{q,k}}{V_{g,k} + \alpha_Q \cdot V_{q,k}} \cdot 100\%$$

Figure 4.14 shows the required increase of bending moment resistance ($\Delta R_{M,req}$) for all analyzed bridges in one platooning scenario. Different colors are used for different bridge types (see Figure 3.15 for bridge type abbreviations); solid lines are used for present resistance level of $\alpha_Q = 1$, dash-dot lines for $\alpha_Q = 0.9$, and dashed lines for $\alpha_Q = 0.8$. Figure 4.15 shows the results for the required increase of shear force resistance ($\Delta R_{V,req}$). Values below 0% mean that no measures are needed.

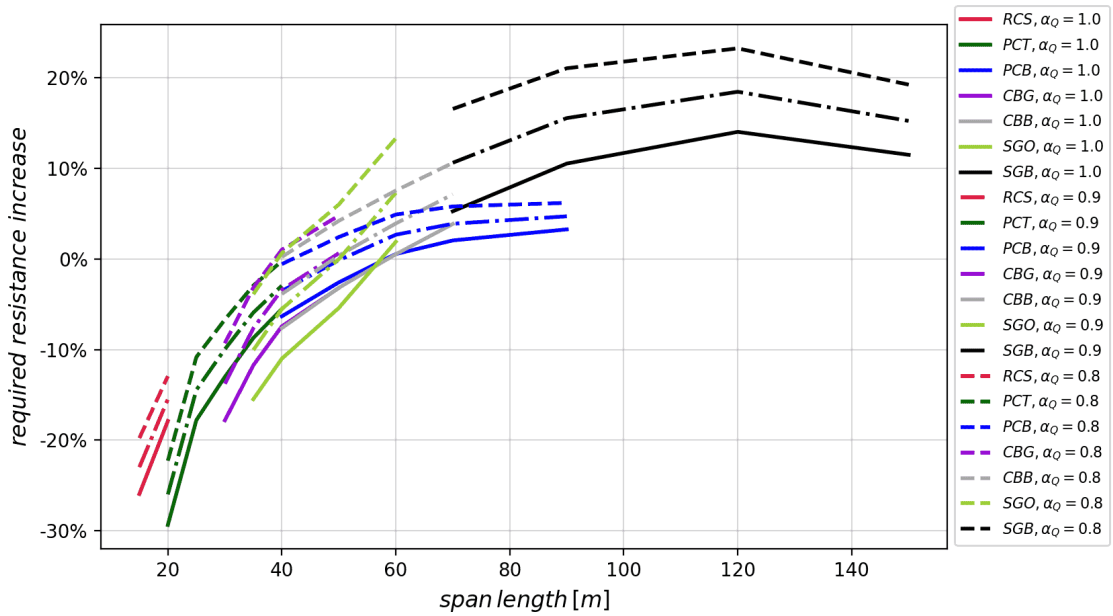

Figure 4.14: Required increase of bending moment resistance in the traffic scenario with 60% platooning penetration rate, constant distances in congestion (C_5), P_{cong}=0.99 and traffic volume of 39000 vehicles/day.

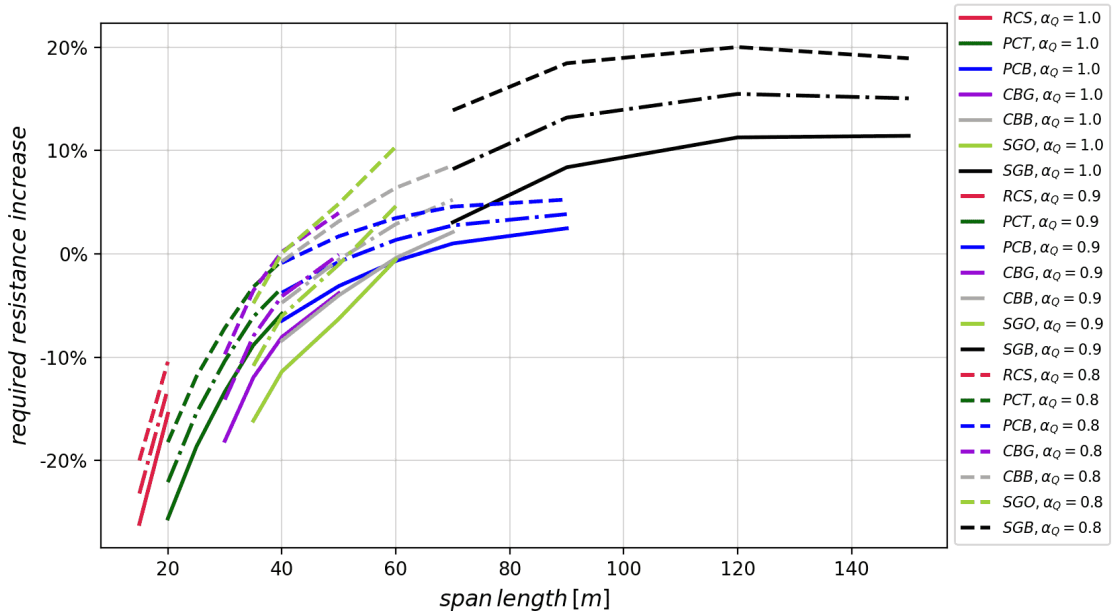

Figure 4.15: Required increase of shear force resistance in the traffic scenario with 60% platooning penetration rate, constant distances in congestion (C_5), P_{cong}=0.99 and traffic volume of 39000 vehicles/day.

The required resistance increase in terms of percent depends also on the permanent loads of the bridge. Bridges, where the permanent load represents a large portion of the total load, are less affected by the increase of traffic loads. This applies to concrete bridges, which are heavy. Light bridges (i.e., steel bridges) are more affected by the traffic load increase.

Further, the required resistance increase depends also on the present bridge resistance. Bridges that are able to carry only 90% or 80% of LM1 load model require a larger resistance increase, if they should be able to carry the new traffic loads on a level that has an exceedance probability of 5% in 50 years. The results shown in Figure 4.14 and Figure 4.15 presume that an exceedance probability of 5% in 50 years should be guaranteed.

Observing the result shown above, it can be concluded that strengthening need would arise for existing bridges with $\alpha_Q = 1$ starting from span length of 55 m for bending moment and 60 m for shear force ULS. Existing bridge with resistance at level of $\alpha_Q = 0.8$, strengthening needs would arise sooner – starting from bridge spans of 40 m.

Limitations

It has to be noted that the results presented above were evaluated for simply-supported single-span bridges with dimensions that were regarded as typical for particular bridge types. Results for actual bridge structures may deviate, as each bridge is different. The presented results are intended to provide an indication only.

Costs

In the next step, an estimate of cost required for the bridge strengthening should be attempted. For this, the results presented above are combined with the cost assumptions shown in Figure 3.9. This results in rough cost estimates shown in Figure 4.16.

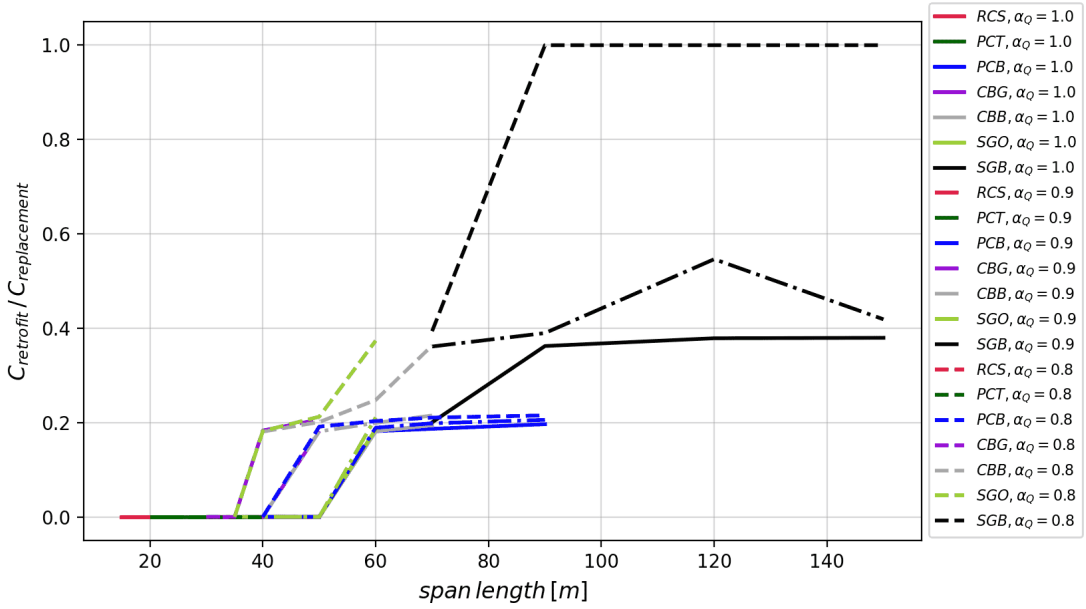

Figure 4.16: Rough cost estimates of required resistance increase in relation to cost of bridge replacement.

The resulting cost estimates concentrate mainly around four levels:

- 0 % of bridge replacement cost – no measures needed,
- 20 % of bridge replacement cost – smaller strengthening measures,
- 40 % of bridge replacement cost – large strengthening measures,
- 100 % of bridge replacement cost – strengthening is not feasible.

As already mentioned, these results must be understood to provide an indication only and may vary depending on the actual bridge structure.

4.2.3 Intelligent access control

The previous chapter presented the option of bridge strengthening to deal with the increased traffic load requirements. Depending on the composition of the bridge population on particular road sections, it could lead to high cost. This applies mainly to bridges with larger span lengths.

To avoid these costs, the option of intelligent access control is introduced. This system presumes communication between truck platoons and the road administration. The basic idea is that platoons should dynamically adjust their inter-vehicle distances depending on the load-carrying capacity of bridges ahead of them, to prevent overloading of the bridges. In the implementation, the road should be divided into sections, and one required inter-vehicle distance should be prescribed for each road section. This value should be governed by the most unfavourable bridge structure in each road section, which is probably the bridge with the largest span. The value of the prescribed vehicle distance valid for current road section must then be communicated to truck platoons as they are travelling across different road sections. The communication of this information could be executed in real-time, or alternatively it could be provided prior to the journey for a selected route or parts of the road network.

To evaluate the required inter-vehicle distances, the bridge response simulations were repeated for different values of inter-vehicle distances within platoons. Table 4.7 summarizes the used cases of vehicle distances.

Table 4.7: Analyzed inter-vehicle distances within platoons.

Distribution	Mean d_μ	Standard deviation	Minimum	Maximum
normal	0.5 m	0.1 m	0.2 m	0.8 m
normal	1 m	0.15 m	0.55 m	1.45 m
normal	2 m	0.2 m	1.4 m	2.6 m
normal	3 m	0.25 m	2.25 m	3.75 m
normal	5 m	0.35 m	3.95 m	6.05 m
normal	7 m	0.45 m	5.65 m	8.35 m
normal	10 m	0.6 m	8.2 m	11.8 m

Figure 4.17 shows the results of exceedance probabilities for the bending moment ULS. The change of inter-vehicle distances has a significant effect on the exceedance probabilities, and thus on the structural safety. Figure 4.18 shows the similar evaluation for the shear force ULS.

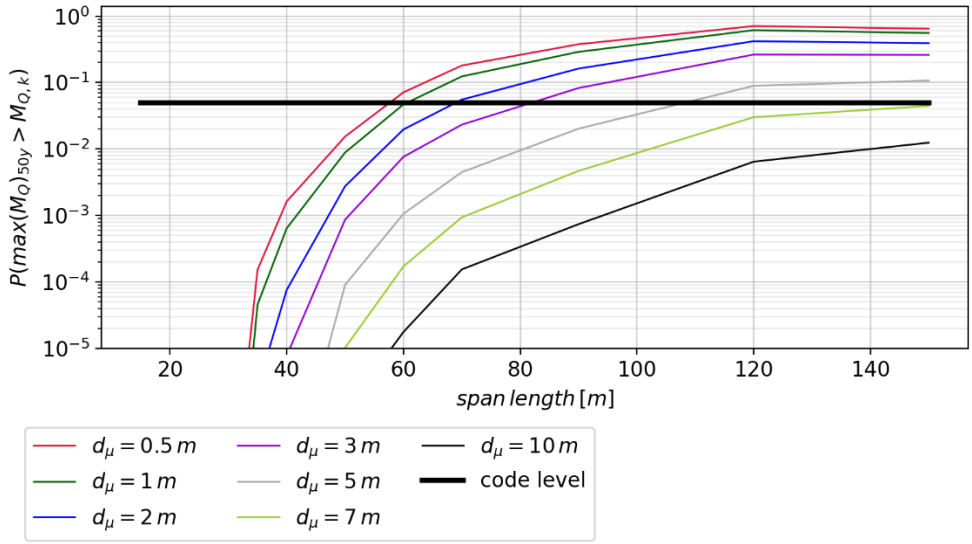

Figure 4.17: Bending moment exceedance probabilities for traffic mix A, traffic volume of 39000 vehicles/day, platooning penetration rate 60%, congestion distances $\mathcal{N}(10,5)$, P_{cong}=0.99, and different inter-vehicle distances within platoons.

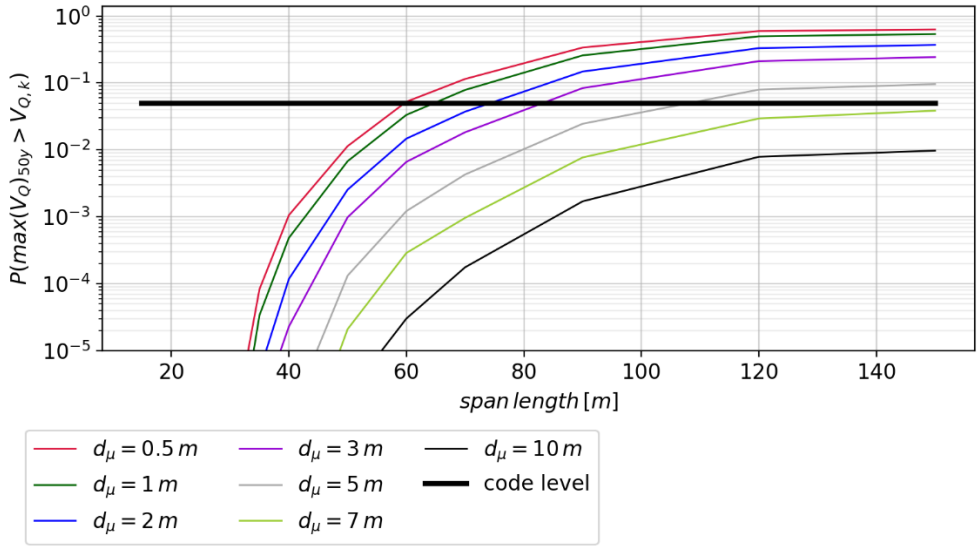

Figure 4.18: Shear force exceedance probabilities for traffic mix A, traffic volume of 39000 vehicles/day, platooning penetration rate 60%, congestion distances $\mathcal{N}(10,5)$, P_{cong}=0.99, and different inter-vehicle distances within platoons.

The results can be used to determine the required inter-vehicle distance for specific length of bridge span. The exceedance probability should remain below 0.05. From this requirement and the results shown above, required vehicle distances listed in Table 4.8 follow. As shown in field tests and wind tunnel tests (Tsugawa et al. 2016), truck platoons with an inter-vehicle distance of 10m still offers energy savings of 15% - 20% for the follower trucks. These savings decrease with distances of >20m. Therefore, we conclude that forcing an increased inter-vehicle distance will not diminish the ecological and economic benefits of truck platoons.

In the application to a road section, the longest bridge span that occurs in that section would be selected and inter-vehicle distance corresponding to this bridge would be prescribed for the whole section.

Table 4.8: Required inter-vehicle distances of platoons in intelligent access control.

Bridge span length [m]	Required inter-vehicle distance [m]
< 55 m	0.5 m
55 – 60 m	1 m
60 – 66 m	2 m
66 – 80 m	3 m
80 – 105 m	5 m
105 – 150 m	7 m
> 150 m	10 m

Congestion

The basic measure of intelligent access control is to increase the inter-vehicle distance of truck platoons before entering the bridge. Although there are other possibilities for handling the platoon if the bridge has more than one lane (e.g., increasing the splitting up the platoon in two lanes, or merging passenger cars into the platoon), we only consider the basic variant since it is the easiest and the most practicable one.

The congestion caused by intelligent access control is evaluated based on the time required to break and reform a truck platoon, i.e., extending the inter-vehicle distances before the bridge and reclaiming the platooning distance afterwards. In any case, this process takes time and causes delay to the traffic on the lane where the platoon operates. The delay mainly depends on the length of the platoon, the change of the inter-vehicle distance and the cruising speed of the platoon.

The process for extending the distance can be regarded as follows. The first truck in the platoon maintains the cruising speed and all follower trucks decelerate until distance between the first and second truck reaches the desired distance. Then the second truck regains the original cruising speed. After the distance between the second and third truck reaches the desired distance, the third truck regains the original cruising speed, and so forth. The process of reforming the platooning is analogous. The first truck decelerates until the gap to the second truck is reduced to platooning distance. Then the second truck decelerates, and so forth.

Depending on the magnitude of deceleration, the process of breaking up the platoon and reforming it will be slow and smooth, or fast but abrupt. Over the whole distance of the operation, the total delay is invariant. For the calculation, we take the difference of the total gap distance between all trucks in platooning formation and after breaking it. This distance needs to be covered by the cruising speed (i.e., we assume that the deceleration brings the trucks to 0 km/h). For simplicity, we assume that the original inter-vehicle distance of the platoon d_μ is 0.5 m. We assume that all trucks in the platoon carry 40ft containers and have a length of 18 m.

The results for the congestion are shown in Table 4.9. The columns indicate the number of trucks in the platoon, the target inter-vehicle distance d_μ for the bridge, the total gap length between the trucks after reaching the target d_μ, the total platoon length including the trucks, the time for breaking or reforming the platoon, and the congestion caused.

Note that this calculation only provides a lower bound for the actual congestion since it is based on theoretical reasoning. In practice, some overhead in the manoeuvre is unavoidable, even if all AV trucks are fully equipped with CACC.

Table 4.9: Delay (s/km) caused by intelligent access control for 50 km/h and 80 km/h cruising speed.

#Trucks in the platoon	Target d_μ	Total gap length	Total platoon length	**50km/h cruising speed**		**80km/h cruising speed**	
				Time for operation	**Congestion (s/km)**	Time for operation	**Congestion (s/km)**
5	1 m	2.5 m	92.5 m	0.18 s	**1.9**	0.1 s	**1.2**
	2 m	7.5 m	97.5 m	0.54 s	**5.5**	0.3 s	**3.5**
	3 m	12.5 m	102.5 m	0.9 s	**8.8**	0.6 s	**5.5**
	5 m	22.5 m	112.5 m	1.62 s	**14.4**	1.0 s	**9.0**
	7 m	32.5 m	122.5 m	2.34 s	**19.1**	1.5 s	**11.9**
	10 m	47.5 m	137.5 m	3.42 s	**24.9**	2.1 s	**15.5**
10	1 m	5 m	185 m	0.36 s	**1.9**	0.2 s	**1.2**
	2 m	15 m	195 m	1.08 s	**5.5**	0.7 s	**3.5**
	3 m	25 m	205 m	1.8 s	**8.8**	1.1 s	**5.5**
	5 m	45 m	225 m	3.24 s	**14.4**	2.0 s	**9.0**
	7 m	65 m	245 m	4.68 s	**19.1**	2.9 s	**11.9**
	10 m	95 m	275 m	6.84 s	**24.9**	4.3 s	**15.5**
15	1 m	7.5 m	277.5 m	0.54 s	**1.9**	0.3 s	**1.2**
	2 m	22.5 m	292.5 m	1.62 s	**5.5**	1.0 s	**3.5**
	3 m	37.5 m	307.5 m	2.7 s	**8.8**	1.7 s	**5.5**
	5 m	67.5 m	337.5 m	4.86 s	**14.4**	3.0 s	**9.0**
	7 m	97.5 m	367.5 m	7.02 s	**19.1**	4.4 s	**11.9**
	10 m	142.5 m	412.5 m	10.26 s	**24.9**	6.4 s	**15.5**
20	1 m	10 m	370 m	0.72 s	**1.9**	0.5 s	**1.2**
	2 m	30 m	390 m	2.16 s	**5.5**	1.4 s	**3.5**
	3 m	50 m	410 m	3.6 s	**8.8**	2.3 s	**5.5**
	5 m	90 m	450 m	6.48 s	**14.4**	4.1 s	**9.0**
	7 m	130 m	490 m	9.36 s	**19.1**	5.9 s	**11.9**
	10 m	190 m	550 m	13.68 s	**24.9**	8.6 s	**15.5**

5 Conclusion and future work

5.1 Conclusions

In this deliverable, micro-simulation was applied to assess the impacts on congestion for automated urban delivery, automated consolidation and hub-to-hub automated transport. The results confirm the assumption that freight traffic has only a small effect on the overall congestion in urban environment since their share of the traffic volume is minimal. For the SUCs automated urban delivery and automated consolidation, the impact on congestion caused by the changes in the delivery procedure is not statistically significant. Nevertheless, an obvious advantage of automated freight transport is the ability to utilise the off-peak hours and the night-time, therefore giving passenger transport more space during the peak hours and reducing some tension. This is in line with the findings in Jennings et al. (2019) and Figliozzi et al. (2020), where the on-road travel could be significantly reduced in scenarios where the service areas are near to the depot. Although the simulation was not performed on the full city level, the delivery area and the delivery route were modelled as realistic as possible. For the hub-to-hub automated transport SUC, the impact is visible, but only if the small area around the transfer hub is considered. On the full city level, the difference would perish as well.

Truck platooning on urban highway bridges is a special SUC in a sense that the assessment methods and the obtained impacts are different from the other SUCs. This SUC is for study purpose and will not be included into the PST estimator, but nevertheless it has an eminent importance. For truck platooning, there already exist a good amount of scientific work, but the impacts on the bridge infrastructure is under-researched. Although the damage is not a short-term effect and the probability of a potential failure is not high, we have to be aware that if a failure occurs, the consequences are disastrous (c.f. Caprigliola bridge collapse, 2020). Therefore, two measures for dealing with the upcoming truck platoons enabled by CCAM are discussed. The results indicate for intelligent access control the necessary increase of inter-vehicle distances for the bridge section to meet the code level. For bridge strengthening, a model and guideline for estimating the costs in relation to the initial construction costs are given. Note that the economical and environmental impacts by truck platooning such as fuel savings are well-researched topics (Humphreys et al. 2016) and therefore not the scope of this report.

5.2 Future work

Since the micro-simulation was only applied on the model of a small network area, a full city model could be used in future work to verify the upscaled results. Similar to D7.2, the question of transferability remains where the goal is to find out the similarities and differences when the method is applied to multiple cities.

For the platooning on urban highway bridges SUC, we used standard bridge models and a standard traffic model to demonstrate the applied methods. In the next step, a case study based on a specific route will be used to calculate specific results and key findings. Also, the question arises if CCAM would cause the freight transport to shift towards smaller vehicles, which would then dampen the problem caused by platooning.

References

Jennings, D., Figliozzi, M. (2019). Study of Sidewalk Autonomous Delivery Robots and Their Potential Impacts on Freight Efficiency and Travel. Transportation Research Record: Journal of the Transportation Research Board, 2673(6), 317–326.

Figliozzi, M. and Jennings, D. (2020). Autonomous delivery robots and their potential impacts on urban freight energy consumption and emissions. Transportation Research Procedia. 46. 21-28.

Baum, L., Assmann, T., Strubelt, H. (2019). State of the art - Automated micro-vehicles for urban logistics. IFAC-PapersOnLine, Volume 52, Issue 13, 2455-2462.

Dorling, K., Heinrichs, J., Messier, G. G., and Magierowski, S. (2017). Vehicle Routing Problems for Drone Delivery. In IEEE Transactions on Systems, Man, and Cybernetics: Systems, vol. 47, no. 1, pp. 70-85.

Allen, J., Browne, M., Woodburn, A., Leonardi, J. (2012) The Role of Urban Consolidation Centres in Sustainable Freight Transport, Transport Reviews, 32:4, 473-490.

Quak, H., Nesterova, N., van Rooijen, T., and Dong, Y. (2016). Zero emission city logistics: current practices in freight electromobility and feasibility in the near future. Transportation Research Procedia, 14, 1506-1515.

Charisis, A., Spana, S., Kaisar, E., and Du, L. (2020). Logistics hub location-scheduling model for inner-city last mile deliveries. International Journal for Traffic & Transport Engineering, 10(2), 169-186.

Cramer, W., Mang, C., McDonnell, A., Nefores, S., Weisman, L. (2020). The impact of automation on shipping and receiving. Proceedings of the International Annual Conference of the American Society for Engineering Management.

Berger, R. (2016). Automated Trucks - The next big disruptor in the automotive industry?

Novak, G. (2016). Autonomous Trucking – The Disruptions on Logistics Value Chain.

Tsugawa, S., Jeschke, S. and Shladover, S. E. (2016). A Review of Truck Platooning Projects for Energy Savings. In IEEE Transactions on Intelligent Vehicles, vol. 1, no. 1, pp. 68-77.

Humphreys, H., Batterson, J., Bevly, D., and Schubert, R. (2016). An Evaluation of the Fuel Economy Benefits of a Driver Assistive Truck Platooning Prototype Using Simulation, SAE Technical Paper.

Sayed, S. M., Sunna, H. N., and Moore, P. R. (2020). Truck platooning impact on bridge preservation. Journal of performance of constructed facilities, 34(3), 04020029.

Braml T. (2010). Zur Beurteilung der Zuverlässigkeit von Massivbrücken auf der Grundlage der Ergebnisse von Überprüfungen am Bauwerk (Reliability assessment of concrete bridges based on the results of bridge inspections), PhD thesis, Universität der Bundeswehr München.

Sedlacek G. (2008). Background document to EN 1991- Part 2 - Traffic loads for road bridges – and consequences for the design.

Freundt, U., Böning, S. (2011). Anpassung von DIN-Fachberichten „Brücken" an Eurocodes (Adaptation of DIN technical reports "Bridges" to Eurocodes), Berichte der Bundesanstalt für Straßenwesen (Reports of the Federal Highway Research Institute), Brücken- und Ingenieurbau Heft B 77 (Bridges and Engineering Construction issue B 77), ISBN 978-3-86918-108-0, Bergisch Gladbach, Germany.

Dimitrios Kalakos, Bernhard Westerhof (2017). Heavy Vehicle Braking using Friction Estimation for Controller Optimization, master thesis at KTH Royal Institute of Technology, School of Engineering Sciences, Stockholm, Sweden.

Elvik, R., Meyer, S. F., Hu, B., Ralbovsky, M., Vorwagner, A., Boghani, H. (2020). Methods for forecasting the impacts of connected and automated vehicles, Deliverable D3.2 of the H2020 project LEVITATE.

Hu, B., Zwart, R.d., Papazikou, E., Boghani, H.C., Filtness, A., Roussou, J., (2019). Defining the future of freight transport, Deliverable D7.1 of the H2020 project LEVITATE.

Hu, B., Brandstätter, G., Ralbovsky, M., Kwapisz, M., Vorwagner, A., Zwart, R.d., Mons, C., Weijermars, W., Roussou, J., Oikonomou, M., Ziakopoulos, Chaudhry, A., Sha, S., Haouari, R., Boghani, H.C., (2021). Short term impacts of CCAM on freight transport, Deliverable D7.2 of the H2020 project LEVITATE.

Hu, B., Brandstätter, G., Ralbovsky, M., Kwapisz, M., Vorwagner, A., Zwart, R.d., Mons, C., Weijermars, W., Roussou, J., Oikonomou, M., Ziakopoulos, Chaudhry, A., Sha, S., Haouari, R., Boghani, H.C., (2021). Medium term impacts of CCAM on freight transport, Deliverable D7.3 of the H2020 project LEVITATE.

Hu, B., Brandstätter, G., Ralbovsky, M., Kwapisz, M., Vorwagner, A., Zwart, R.d., Mons, C., Weijermars, W., Roussou, J., Oikonomou, M., Ziakopoulos, Chaudhry, A., Sha, S., Haouari, R., Boghani, H.C., (2021). Long term impacts of CCAM on freight transport, Deliverable D7.4 of the H2020 project LEVITATE.